Synthesis and Phase Behavior of End-Functionalized Associating Polymers

by

Michelle H. Wrue

Submitted in Partial Fulfillment
of the
Requirements for the Degree of

Doctor of Philosophy

Supervised by
Professor Mitchell Anthamatten

Department of Mechanical Engineering

Materials Science Program

Arts, Sciences and Engineering

Edmund A. Hajim School of Engineering and Applied Sciences

University of Rochester

Rochester, NY

2010

Dedication

This thesis is dedicated to:

My parents, Kathi and Rick Horch, for teaching me that I can do anything that I want in life and for their continued encouragement and support in all things.

My beautiful girls, Mackenzie and Melissa, for loving me no matter how much time I spent on school and always running to greet me when I came home.

My husband, Steve, whose unwavering support and unconditional love kept me going more than he knows.

Curriculum Vitae

Michelle Horch Wrue was born in Rochester, New York on January 25, 1975. She attended the State University of New York, College at Brockport from 1993-1997, completing her Bachelor of Science in Chemistry degree in 1997. She began graduate studies at Virginia Polytechnic Institute and State University in 2001, graduating with a Masters of Engineering degree in Materials Science and Engineering in 2003. Michelle came to the University of Rochester in 2003 to pursue further graduate studies in Materials Science. She served as a teaching assistant for the Department of Mechanical Engineering from 2003-2004. She received the Frank J. Horton Fellowship from 2004-2009. She pursued the study of self-associating polymers under the direction of Professor Mitchell Anthamatten and received the Master of Science degree from the University of Rochester in 2005.

Acknowledgements

Many, many people helped to make this thesis a reality. In particular I would like to thank my advisor, Mitch Anthamatten for his guidance in my research. Mitch's synthetic background was particularly helpful in getting this work 'off the ground'. Additionally, Mitch's theoretical and modeling background have been invaluable in the interpretation of my phase behavior observations. Finally, Mitch's patience, understanding and support of a graduate student that is also a parent have made my graduate experience much less stressful than it might have otherwise been. Thank you!

I would also like to thank my officemate of 6 years, Xichong Chen. We started our U of R graduate journey together and I have valued your input, support and most importantly, your friendship. It will be very weird not to see you every morning. Research would have been very lonely without all the other graduate members of the Anthamatten research group as well: Lijun Zou, Jiahui Li, Supacharee Roddecha, Zach Green, Alex Papastrat, Kavya Ramachandra, Chris Lewis and Shuai Zhu. Thank you all for making research enjoyable and (sometimes) a bit of an adventure! I will actually miss our 'lab cleaning days'. All of us in one lab at the same time always led to more than a few laughs.

Thank you to Aaron McUmber for his help with the solvent blend studies during his undergraduate research. I also need to acknowledge my 'solvent daddy', Jason Wallace. Jason's access to unusual solvents and his willingness to share them, along with numerous technical discussions were most helpful in my research.

I am indebted to several people for testing and technical discussions related to my research. Thanks to Anthony Geiss (MALDI-ToF), Chris Pratt (X-ray), Tom Mourey (technical GPC discussions) and Dennis Massa (PS/PMMA blends)

There are many people other than research associates that I need to thank as well. Thanks to: Joe Wodensheck and Chris Bailey for their continued friendship and support; and the Mechanical Engineering office staff (Carla, Jill and Carm) for the guidance, friendship, and help getting my feet wet as a new University of Rochester graduate student.

Thank you to the Chemical Engineering office staff (past and present). Sandra, Andrea, and Tiffany thanks for the friendship, support and for keeping the coffee flowing.

And I would be horribly remiss if I did not thank my friend Anne Miller for pushing me to do this in the first place.

And last, but certainly not least, thanks to my family for their love and support. To my sister, Katie, thank you for being such an incredible 'third parent' to my girls that I was 'ok' with leaving them everyday. I could not have done this without you! Mom and Dad, thank you for making me work for my education. To my husband Steve, and my daughters Mackenzie and Melissa, thank you for allowing me to work for it.

Abstract

We have explored polymer blend phase behavior in the presence of multiple hydrogen bonding end-groups. This work details the synthesis of functionalized polymers and their subsequent use in miscibility studies. The synthesis of end-functionalized hydrogen bonding polymers and the investigation of their physical properties and miscibility is presented. Mono-functional and telechelic ureidopyrimidinone (UPy) functionalized polymers were prepared by two main routes: post-polymerization functionalization (of commercially available or synthesized polymers); and polymerization of monomers using a functionalized initiator. UPy-functionalized polymers were prepared with a variety of polymer backbones including poly(ethylene oxide)s; poly(butadiene)s, poly(dimethyl siloxanxe)s; poly(styrene)s and poly(methyl methacrylate)s. The most successful route to polymers with UPy end-groups was atom transfer radical polymerization (ATRP) using a UPy-functionalized initiator, followed by atom transfer radical coupling (ATRC).

The incorporation of ureidopyrimidinone end-groups was shown to affect the physical properties of the polymer backbone. Parent polymers that were liquids became viscous liquids or waxy solids upon UPy-functionalization of chain end. UPy-functionalization of a hydroxyl-terminated polybutadiene (HO-PB-OH) resulted in a waxy solid while the HO-PB-OH precursor was a viscous liquid. The thermal properties of functionalized polymers also differed from those of the unfunctionalized parent polymers. Hot-stage optical microscopy revealed that UPy-functionalized

PEO displayed a depressed melting point relative to the analogous unfunctionalized precursor. Differential scanning calorimetry was also used to investigate the synthesized UPy-polymers. UPy-functionalized polystyrenes and poly(methyl methacrylate)s showed an increased T_g compared to the equivalent homopolymer standards. This increased T_g was determined to be dependent upon the fraction of UPy groups present and chemical cleavage of the end-groups resulted in T_gs near those observed for polymer standards of comparable molecular weight.

Aggregation of UPy end-groups in solution was observed using gel permeation chromatography. Aggregation was only observed for telechelic samples of low molecular weight, indicating that the aggregation of end-groups is dependent upon the concentration of the end-groups.

The effect of UPy end-groups on blend miscibility was studied in solution using laser light scattering and in the melt state was using laser light scattering, optical microscopy and differential scanning calorimetry. The incorporation of associating groups onto one end of either blend component decreases miscibility relative to the unfunctionalized parent blends. Lower miscibility was also observed for blends in which both components were mono-functionalized with associating end-groups. The largest decrease in miscibility was observed for blends containing telechelic UPy-functionalized polymers, which were immiscible across the entire composition range.

Table of Contents

List of Tables

List of Figures

List of Symbols

A	acceptor (in hydrogen bonding)
2-AHMP	2-amino-4-hydroxy-6-methylpyrimidone
ATR	attenuated total reflectance (FT-IR spectroscopy)
ATRP	atom transfer radical polymerization
ATRC	atom transfer radical coupling
BMP	2-bromo-2-propionic acid
^{13}C NMR	carbon nuclear magnetic resonance
$^{\circ}$C	degrees Celsius
χ_{ij}	Flory Huggins interaction parameter
$CDCl_3$	deuteratred chloroform
$CHCl_3$	chloroform
Δ	heat (when symbol used alone)
D	donor (in hydrogen bonding)
DBTDL	dibutyltin dilaurate
DCC	dicyclohexyl carbodiimide
DCM	dichloromethane
DMAP	dimethylaminopyridine
DMF	*N*,*N*-dimethylformamide
DMSO	dimethyl sulfoxide
DP	degree of polymerization
DSC	differential scanning calorimetry
ϕ_i	volume fraction of i component
FT-IR	Fourier transform infrared spectroscopy
ΔG_m	Gibb's free energy of mixing
ΔG_H	Gibb's free energy due to H-bonding
GPC	gel permeation chromatography
H-bonding	hydrogen bonding
HCl	hydrochloric acid
HDI	hexyldiisocyanate
^{1}H NMR	proton nuclear magnetic resonance
HEBrIBu	2-hydroxyethyl-2-bromoisobutyrate
HPLC	high performance liquid chromatography
hr	hour
K	equilibrium constant
K_a	equilibrium association constant
k_a	activation rate (ATRP)
k_d	deactivation rate (ATRP)
k_p	propagation rate (ATRP)
k_t	termination rate (ATRP)
L	ligand (ATRP)
LCST	lower critical solution temperature

M	monomer (ATRP)
MALDI-ToF	Matrix assisted desorption/ionization time of flight mass spectrometry
mg	milligram
min	minute
mL	milliliter
mmol	millimole
M_n	number-average molecular weight
mol	mole
M_w	weight-average molecular weight
n	number of repeat units (polymer chains)
N_i	number of repeat units in i component
Napy	2,7-diamido-1,8-naphthryidines
NCO	isocyanate
NMP	n-methyl pyrrolidinone
NMR	nuclear magnetic resonance
P	polymer (ATRP)
PB	polybutadiene
PCAM	Painter-Coleman association model
PDI	polydispersity index
PDMS	polydimethylsiloxane
PEG	poly(ethylene glycol)
PEO	poly(ethylene oxide)
PMDETA	N,N,N',N",N"-pentamethyldiethylene triamine
PMMA	poly(methyl methacrylate)
PS	polystyrene
R	ideal gas constant
σ	stress
SMBC	supramolecular block copolymer
SMP	supramolecular polymer
T	temperature
T_c	cloud point temperature
T_g	glass transition temperature
T_m	melting temperature
TFA	trifluoroacetic acid
THF	tetrahydrofuran
UCST	upper critical solution temperature
UPy	ureidopyrimidinone
UPy-BrIBu	2-ureidopyrimidinone-ethyl-2-bromoisobutyrate
UPy-NCO	2(6-isocyanatohexylaminocarbonylamine)-6-methyl-4-[1H] pyrimidinone
vpo	vapor pressure osmometry

Chapter One: Introduction & Background

1.1 Supramolecular polymers

Supramolecular polymers (SMPs) are comprised of oligomer units that are held together by reversible, non-covalent bonds[1-6] (Figure 1). Potential reversible alternatives to covalent bonds include: hydrogen bonding, ionic interactions, and metal-ion coordination. Supramolecular polymer structures are dynamic and are always in equilibrium with their environment. This feature enables material properties to be tuned by adjusting environmental conditions, typically temperature, solvent or pH. Several new classes of stimuli-responsive materials, derived from secondary interactions, have recently emerged.[7] Supramolecular polymers are being developed for use as self-healing materials,[8] shape memory polymers[9] and thermoplastic elastomers[10] (Figure 2). Moreover, supramolecular polymers offer a combinatorial approach to changing polymer architecture and material properties. In principle, simple blending of different monomers can be used to adjust/modify material properties.

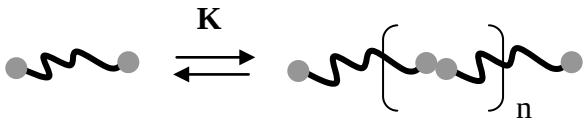

Figure 1: Reversible association of end-groups to form a supramolecular polymer.

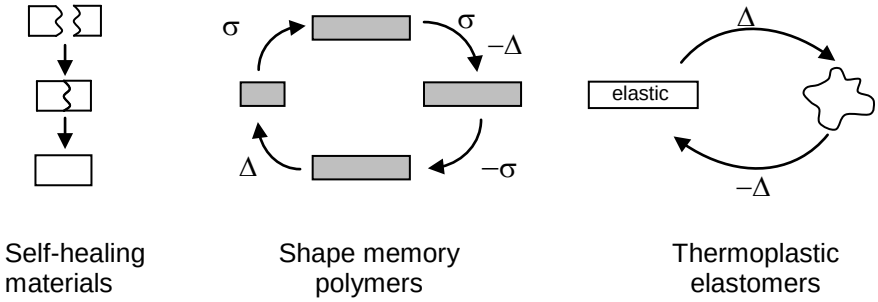

Figure 2: Stimuli-responsive applications of supramolecular polymers. Δ indicates application of heat and σ indicates application of stress.

Commodity polymers require high molecular weights to promote good mechanical properties. However, higher molecular weights can hinder melt processing due to increased melt viscosities and decreased thermal stability. The reversible association of low molecular weight polymers offers a route to gain the desired physical properties at the low temperature "use" state without compromising melt processability. Dissociation of reversible end-groups at elevated temperatures lowers the effective molecular weight, and therefore the viscosity. Subsequent cooling to the end-use temperature results in association, with higher effective molecular weight, and polymer-like behavior.[11] A similar concept has enabled the creation of new thermoplastic elastomers.[12] For example, the incorporation of hydrogen bonding end-groups onto poly(ethylene butylene) results in an elastic solid at room temperature, whereas the unfunctionalized polymer is a viscous liquid.[13]

1.2 Hydrogen bonded supramolecular polymers

Hydrogen bonding interactions have played a significant role in the development of SMPs.[2, 14-17] Polymer-like properties have been reported, in solution and the bulk state, through H-bonding association of low molecular weight oligomers.[2, 14, 16] Of particular interest to polymer processing considerations is the temperature dependence of hydrogen bonds.

Hydrogen bonds are dynamic and exist in equilibrium between associated and dissociated states. Hydrogen bond strength is influenced by numerous parameters including: temperature, humidity, solvent choice, concentration, conformation/steric hindrance, acid/base character of the donor and acceptor,[18] and number of hydrogen bonds formed. The arrangement of hydrogen bonds in multiple H-bonding complexes affects bond strength as well. Hydrogen bonding groups with the same number of hydrogen bonds can have very different strengths and stabilities. For example, the arrangement of donors (D) and acceptors (A) within the hydrogen bonding moiety determines if secondary interactions are attractive or repulsive (Figure 3). Limiting the occurrences of repulsive secondary interactions can result in greater stability and bond strength.[19, 20]

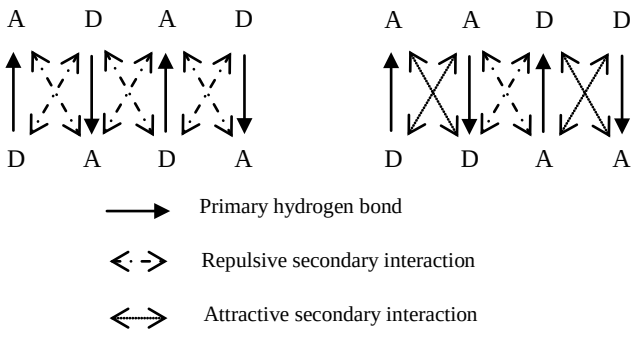

Figure 3: Secondary interactions in multiple hydrogen bonding groups.

Hydrogen bonding groups are classified according to their ability to self-associate. Groups that are able to hydrogen bond with themselves are termed "self-complementary". Groups that only associate with a separate, complementary group are referred to as "hetero-complementary". Figure 4 shows examples of each type of hydrogen bonding group.

Figure 4: Self-complementary (A) and hetero-complementary (B) hydrogen bonding groups.

Hydrogen bonding motifs can be designed to promote association. Early development of hydrogen-bonded supramolecular polymers utilized functional groups that formed associations using one, two or three hydrogen bonds. These materials exhibited association constants (K_a) less than 10^3 M^{-1}. [2] Motifs containing more hydrogen bonding sites increase the overall strength of the interaction while enhancing its specificity. Multiple H-bonding groups[14] have been recently developed that utilize four,[21-26] six[27] and eight[28] hydrogen bonding sites. Meijer's group has synthesized and investigated telechelic supramolecular polymers functionalized with ureidopyrimidinone (UPy) end-groups.[21-24] The UPy group contains four hydrogen bonding sites arranged in a donor-donor-acceptor-acceptor (DDAA) arrangement (Figure 4A). These self-complementary groups exhibit an association constant in chloroform greater than 10^6 M^{-1}. [23]

1.3 Polymer miscibility

Polymer blending plays a vital role in the development of new materials with tunable properties and easier processing.[29-31] Polymer blends can exhibit complete miscibility, complete immiscibility or conditional miscibility. Conditionally miscible materials show a dependence on factors such as blend composition and temperature (Figure 5). Conditional miscibility behavior can be divided into two categories based on the temperature dependence of the system. Blends that are miscible at a given temperature and phase separate upon subsequent heating are referred to as exhibiting a lower critical solution temperature (LCST). Blends that are miscible at a given

temperature and phase separate upon subsequent cooling are referred to as exhibiting an upper critical solution temperature (UCST). The temperature at which a given blend composition phase separates is termed the cloud-point temperature T_c. When a single cloud-point temperature is reported for a blend, the highest (for UCST) or lowest (for LCST) of the measured phase boundary is usually reported.

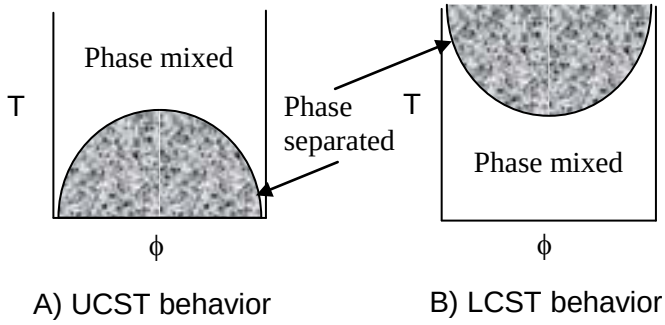

Figure 5: Depiction of upper and lower critical solution temperature behaviors. Shaded areas indicate presence of two separated phases.

UCST behavior can be explained by traditional Flory-Huggins theory which utilizes a simple lattice model to develop predictions for ΔG_m of polymer blends.[32] The common form of the Flory-Huggins equation is:

$$\frac{\Delta G_m}{RT} = \left(\frac{\phi_A}{N_A} \ln \phi_A + \frac{\phi_B}{N_B} \ln \phi_B + \chi_{AB} \phi_A \phi_B \right) \qquad [1]$$

where R is the gas constant, T is the absolute temperature, ϕ_A, ϕ_B and N_A, N_B, are the volume fractions and degrees of polymerization of polymers A and B, respectively, and χ_{AB} is the Flory-Huggins interaction parameter for A interacting with B.

Equation 1 considers changes in enthalpy and entropy upon mixing. The first two terms on the right hand side of Equation 1 account for combinatorial entropy which, while favorable for mixing, is only a small contribution for polymer blends. The last term is an enthalpic term and its magnitude is largely indicative of whether or not two polymers will form a single mixed phase.

Compared to traditional polymer-polymer blends, one would expect phase behavior to differ for blends containing supramolecular polymers. Traditional Flory-Huggins theory is not sufficient for the prediction of miscibility of blends containing supramolecular polymers for several reasons. The enthalpic interaction of reversibly-associating end-groups can lower the free energy of the blended state. This association includes an entropic free energy penalty as well. At temperatures where association is not favored, the SMP will be present not as a long chain, but as shorter oligomer units which should promote the formation of a single phase. Flory-Huggins theory does not account for such reversible associations.

Specific interactions between the functional groups of SMPs can lead to local ordering and thus a non-random distribution of molecules. Flory-Huggins theory assumes random ordering of the blend. Also, Flory-Huggins theory assumes blend incompressibility and the interaction parameter considers only *combinatorial* entropy. Non-combinatorial entropy arises from changes in volume upon mixing. This non-combinatorial entropy dominates over enthalpy at elevated temperatures. However, at elevated temperatures, hydrogen bonding is less favored, so the contribution from non-combinatorial entropy for H-bonded SMPs is a complex issue.

1.4 Miscibility of polymers containing hydrogen bonding groups

1.4.1 Miscibility of polymers with H-bonding side-groups

Hydrogen bonding between polymer blend components can enhance miscibility.[33-38] There are many examples in the literature that illustrate this phenomenon. Viswanathan et al. report miscibility between liquid crystalline polyurethane and amorphous polystyrene-co-poly(vinylphenol) through the use of hydrogen bonding groups distributed along the backbones of the blend components.[39, 40] Park and Zimmerman have used hydrogen bonding side-groups to impart miscibility to usually immiscible blends of polystyrene with poly(butylmethacrylate).[39] Cowie et al observed an increase in the LCST of poly(vinylmethyl ether)/poly(α-methylstyrene) blends when hydrogen bonding was incorporated.[41]

Thermodynamic models have been developed to predict the phase behavior of blends that undergo hydrogen bonding of side-groups.[34, 42, 43] The model developed by Painter and Coleman,[34] shown in Equation 2 below, is a modification of traditional Flory-Huggins theory to account for the change in free energy due to intermolecular hydrogen bonding of side-groups. The additional free energy term accounts for the change in Gibbs free energy when hydrogen bonds are formed in the blend.

As discussed above, the first two terms in Equation 2, arising from combinatorial entropy, are favorable to mixing but the magnitude of these terms is

largely negligible for polymer blends. Miscibility in hydrogen bonded mixtures will therefore depend on the balance between the third and forth terms of the equation. The favorable contribution to mixing from the hydrogen bonding term will depend on both the magnitude of self-association versus inter-association as well as the volume fraction of associating groups in the blend. This additional term accounts for the ΔG_m contribution due the creation of *new* hydrogen bonds upon mixing. The number of new bonds formed depends on the number of free and bound side-groups present prior to mixing and the association constant of the side-group.

$$\frac{\Delta G_m}{RT} = \left(\frac{\phi_A}{N_A} \ln \phi_A + \frac{\phi_B}{N_B} \ln \phi_B + \chi_{AB} \phi_A \phi_B \right) + \frac{\Delta G_H}{RT} \qquad [2]$$

The Painter-Coleman association model (PCAM) has been successfully applied to several polymer blends.[33, 44-46] Discrepancies between PCAM predictions and experimental results can be attributed to the non-ideality of "real" polymer blends.[47] The Painter-Coleman model makes several assumptions that may not apply to "real" blend systems:

- random mixing
- blend components are roughly same size and shape
- free volume changes are neglected
- chains are highly flexible

Additionally, the PCAM does not consider blends in which both components can *self*-associate through hydrogen-bonding.

1.4.2 Miscibility of polymers with H-bonding end-groups

The use of associating end-groups provides several advantages over associating side-groups for the enhancement of polymer blend miscibility. Association of *end-groups* typically results in the formation of linear structures; while association of *side-groups* can lead to the formation of branched or network-like structures. While, the aggregation of hydrogen bonding *end-groups* into stack like structures has been reported,[48] the potential for this type of structure is decreased relative to polymers with associating side-groups. The existence of branching and/or network structures can result in decreased blend miscibility.[49-51] End-groups also have increased mobility compared with side-groups and are their ability to form associations is less likely to be affected by backbone rigidity and steric hindrance than associating side-groups. All of these factors increase the likelihood that association will occur in end-functionalized polymers.

Although there are many studies on the effect of hydrogen bonding on blend phase behavior, the majority of published findings (like those discussed above) are limited to hydrogen bonding *side-groups.* Few studies in the literature address the affects of hydrogen bonding *end-groups* on polymer miscibility.[35, 52] Associating end-groups can strongly affect polymer miscibility. Haraguchi et al reported a destabilization of the two phase region of the phase diagram for blends of carboxylated PS and aminated PEG when the functionality was introduced to one end of each blend component. [35] Results indicate that due to cross-association, carboxylic acid dimers are disrupted when basic amino acid groups are introduced.

There are several published studies showing the incorporation of hydrogen bonding groups resulting in block copolymer structures.[53-57] Park and Zimmerman reported the preparation of multi-block copolymers using hydrogen bonding end-groups.[53] The degree of polymerization was controlled through concentration and ratio of blocks present. Yang et al utilized hetero-complementary 6-membered hydrogen bonding end-groups to create an AB diblock copolymer of PS and PEG.[54] Supramolecular copolyesters with tunable properties have been prepared by blending homopolymers with self-complementary end-groups.[56]

The Painter-Coleman model has been recently extended to consider polymer blends that contain reversibly associating end-groups.[58] Here, consideration is given to both monofunctional and telechelic polymers. Additionally, self-complementary and hetero-complementary end-groups are considered. As expected, this model predicts that self-association of one component always stabilizes the two phase region of the phase diagram. The shape of the predicted phase diagram changes as a function of temperature. At low temperatures, where self-association dominates, the phase diagram is skewed toward the non-associating component. The degree of asymmetry depends on the association constant of the end-groups. At elevated temperatures, end-group association is decreased and the phase diagram returns to the symmetric shape predicted by traditional Flory-Huggins theory.

1.5 Intellectual challenges

There is a limited body of experimental work on blends containing supramolecular polymers.[59, 60] Specifically, the effect of multiple hydrogen bonding end-groups in supramolecular polymer blends has not been well studied. Studies of associating polymers have aimed at understanding, fundamentally, how molecular details affect the equilibrium degree of association. As the majority of research has been conducted in solution, there still exists a need to understand association in the melt state and how it differs from solution.

Moreover, the ability to quantitatively predict how association and the presence of hydrogen bonding groups affect miscibility is not well established. Existing models do not consider all contributing factors of phase behavior in these systems.[47] Free volume effects and backbone rigidity/flexibility are often neglected. The molecular weight and rigidity of the polymer can have a significant effect on the phase behavior.[61] In addition to the strength of association, immiscibility of the oligomers between the associating groups must also be considered when discussing phase separation in SMPs. The ability to predict association and phase behavior of these materials is critical to a supramolecular-based approach to creating new materials.

Supramolecular polymers are being developed into thermoplastic elastomers,[10] shape-memory materials[9] and self-healing materials.[8] A more thorough understanding of the kinetics of mixing/demixing and association of supramolecular polymers is clearly important for such applications. Control of the

association/dissociation equilibrium is vital to the use of SMPs as stimuli-responsive materials. For self-healing and shape-memory materials, the ability to tune and control the speed at which equilibrium is achieved may influence surface healing contact times and shape recovery rates, respectively.

The development of supramolecular block copolymers (SMBC) also requires a clearer understanding of association and phase behavior. Connecting dissimilar polymers by associating groups can result in a continuum of phase morphologies including a) complete mixing and formation of a single homogeneous phase, b) mixing with microphase segregation, and c) complete demixing with the formation of separate, distinct phases.[62] Conventional block copolymers utilize microphase separation to achieve desired phase morphologies. In SMBCs the non-covalent attraction between end-groups must be carefully balanced against the repulsion between the two blocks to ensure microphase separation. Several groups have observed microphase separation in supramolecular AB diblock copolymers utilizing hydrogen bonding groups.[54, 55, 63] Also of interest to SMBCs is the ability to tune the association equilibrium to achieve the desired physical properties at use temperatures.

1.6 Objectives of current research

The aim of our research is to experimentally study how the presence of multiple hydrogen bonding end-groups affects the phase behavior of polymer blends. To achieve this, monofunctional and telechelic end-functionalized polymers of have been synthesized. Blends containing these functionalized polymers were prepared

and the resulting phase behaviors were characterized and compared with that of traditional polymer-polymer blends.

The primary issues we hoped to address with this research are as follows:

- How does the incorporation of self-associating end-groups affect the thermal and physical properties of the parent polymers? Are the effects on these properties different for monofunctional and telechelic substituted polymers?
- How does the incorporation of self-associating end-groups affect the phase behavior of polymer blends?
- How does melt and solution phase behavior of a polymer blended with a monofunctional, hydrogen bonding polymer blend compare with that of a polymer blended with a supramolecular (telechelic) polymer?

Chapter Two: Selection of Hydrogen Bonding Group and Polymer Blends

2.1 Selection of hydrogen bonding end-group

Our studies have focused on the self-complementary ureidopyrimidinone hydrogen bonding group. There are several advantages to the selection of this end-group. The UPy group features an AADD arrangement of hydrogen bonds which minimizes the affect of unfavorable repulsive secondary interactions as discussed in Chapter 1. The synthesis of this group is relatively straightforward and is well documented in the literature.[64] Additionally, UPy-containing materials can be blended with materials containing 2,7-diamido-1,8-naphthryidine (Napy) end-groups which have been shown to interrupt the self-association of UPy groups in favor of UPy-Napy complementary interactions.[65] This allows for an easy transition to the study of hetero-complementary hydrogen bonding end-groups in future research.

Monofunctional and telechelic UPy-functionalized polymers have been synthesized for use in blend studies. There are two possible routes to incorporate UPy-functional end-groups onto existing conventional polymers (Figure 6). One approach utilizes a UPy-functionalized isocyanate that can be reacted with a hydroxy group on the polymer chain.[61] The second route uses a UPy-functionalized imidazole that can then react with amine end-groups.[63]

Figure 6: Attachment of UPy groups via a) isocyanate chemistry,[16] and b) imidazole chemistry.[66]

2.2 Blend selection

The blends chosen for miscibility investigations are shown in Table 1. Several criteria were used in the selection of these polymer blends including:

1) Ability to prepare functionalized materials of controlled molecular weight (low polydispersity);
2) Ability of the parent polymers to form a miscible blend;
3) Expected phase transitions at experimentally accessible temperatures;
4) Availability of previous studies of parent blends for comparison;
5) Availability of parent polymer molecular weight standards.

In addition, the selected blends were chosen because they incorporate polystyrene. Sarbu has developed a route to well defined, controlled molecular weight, hydroxyl-

terminated polystyrenes using atom transfer radical polymerization followed by atom transfer radical coupling (ATRP/ATRC).[67] Ureidopyrimidinone end-groups can then be attached using isocyanate chemistry (Figure 6a). Alternatively, the hydroxy-bromoisobutyrate initiator can be functionalized with the UPy group prior to ATRP, guaranteeing functionalization of both terminals of the resulting polymer (Figure 7). The selected blends will be briefly discussed below.

Table 1: Polymer blends selected for miscibility studies.

Blend component A	**Blend component B**	**Phase behavior of parent blend**	**Targeted Blends**
PS	PB	UCST[68-71]	PS/UPy-PB-UPy UPy-PS/PB UPy-PS-UPy/PB UPy-PS-UPy/UPy-PB-UPy
PS	PMMA	UCST at low M_n[72] Immiscible otherwise[73]	UPy-PS/PMMA, PS/UPy-PMMA UPy-PS/UPy-PMMA UPy-PS-UPy/UPy-PMMA-UPy
PS	PDMS	UCST at low M_n Immiscible otherwise[74]	UPy-PS/UPy-PDMS-UPy UPy-PS-UPy/UPy-PDMS-UPy

Figure 7: ATRP/ATRC synthesis of UPy-terminated polystyrene.

Polystyrene/polybutadiene (PS/PB)

Studies of polystyrene (PS)/polybutadiene (PB) blends are numerous,[68-71, 75, 76] largely due to interest from the rubber industry. Styrene and butadiene are commonly used in multiphase commercial polymer materials such as styrene-butadiene rubber and high impact polystyrene. The phase behavior of PS and PB has been thoroughly studied to optimize the behavior of these multiphase materials. Based on these published studies, UCST phase behavior for low molecular weight blend components is expected at experimentally accessible temperatures.

Polystyrene/poly(methyl methacrylate) (PS/PMMA)

Investigations of blends of polystyrene with poly(methyl methacrylate) have been reported by numerous groups.[72, 73, 77-83] Blends with molecular weights above 10,000 g/mol were reported to be immiscible across the entire composition range. However, several groups[72, 83, 84] have reported UCST behavior for blends of low molecular weight materials. Both blend components can be synthesized, with or without UPy end-groups using ATRP/ATRC chemistry.

Polystyrene/poly(dimethyl siloxane) (PS/PDMS)

The unique properties of silicone (heat stability, UV stable, low T_g, good gas permeability)[85] make PDMS very attractive for many applications. However, the[86] poor mechanical properties of PDMS often make the use of reinforcing materials necessary.[86] The incorporation of glassy polymers, such as polystyrene, is one approach to improve mechanical properties. Published attempts at direct mixing of PS with PDMS to create a commercially viable blend have been unsuccessful.[86] While the PS/PDMS system exhibits UCST behavior at very low molecular weights,[74] immiscibility is observed at higher molecular weights.

2.3 Summary

The ureidopyrimidinone (UPy) functionality was chosen to be used as the reversibly associating end-groups for our polymer blend studies. The UPy group is a versatile, self-complementary quadruple hydrogen bonding end-group whose synthesis is well documented in the literature. Several UCST polymer blends incorporating polystyrene were chosen for our blend studies, as UPy-functionalized polymers can be readily synthesized by several methods including ATRP/ATRC.

Chapter Three: Synthesis of Target UPy-functional Materials

The following sections detail the synthetic routes employed to prepare UPy-functionalized polymers for use in our studies. The sections are organized as follows: first, UPy-functionalization of commercially available polymers (PEO, PB and PDMS) by two different routes will be discussed; next, ATRP/ATRC reactions with a hydroxyl-terminated initiator and subsequent UPy-functionalization will be discussed (PS and PMMA); finally, the reactions performed to synthesize a UPy-functionalized initiator and it's use in ATRP/ATRC reactions will be discussed (PS and PMMA). The structures of all prepared polymers are shown in Figure 8.

Details are given for an example reaction of each unique synthetic approach used to prepare to a given functionalized polymer. For polymerization reactions, reaction times, temperatures and reactant ratios were varied to achieve polymers of varying molecular weight. Given the large number of polymerization reactions performed, all these synthetic variations will not be discussed individually. Details of the different reaction conditions and the characteristics of the resulting polymers are given in Appendix A. Unless otherwise stated, all materials are commercially available and were used without further purification.

All prepared materials were characterized individually prior to their use in blend studies. Structure determinations were carried out in deuterated solvents using a Bruker Avance 400MHz NMR spectrometer and in the solid state using a Shimadzu 8400S FT-IR equipped with a diamond ATR stage. Molecular weights of prepared

Figure 8: Structures of synthesized telechelic materials.

*Indicates monofunctional polymer was also prepared.

polymers were measured by GPC. Instrumentation included an Agilent 1100 HPLC system equipped with a Viscotek triple detector. Three columns were utilized (two Viscotek mixed bed, low M_w, i-series and one mixed bed, medium M_w, i-series column). The system temperature was maintained at 60 °C when n-methylpyrrolidinone (NMP) was the mobile phase and 30 °C when tetrahydrofuran (THF) was used. Calibration was performed using polystyrene standards of varying molecular weight. GPC traces were interpreted using the instrument software package OmniSEC (Viscotek).

3.1 Synthesis of UPy-functionalized materials via hydroxyl-terminated oligomers

3.1.1 Synthesis of UPy-functionalized isocyanate (UPy-NCO)

Following the reaction scheme [64] shown in Figure 9, 0.70 mol of 2-amino-4-hydroxy-6-methylpyrimidine (2-AHMP) was added to 4.75 mol twice distilled hexyldiisocyanate (HDI) and the resulting mixture was heated 16 hours at 100 °C. Pentane was added and the reaction mixture was filtered. The filtered precipitate was then washed with additional pentane. The white solid was dried overnight in a 50 °C vacuum oven. FT-IR and proton NMR, shown in Figure 10, confirmed the formation of the desired product, 2(6-isocyanatohexylaminocarbonylamino)-6-methyl-4-[1H] pyrimidinone (UPy-NCO). ^{1}H NMR (400MHz, $CDCl_3$): δ 13.1(s,1H, CH_3-C-N<u>H</u>), 11.9 (s, 1H, CH_2-NH-(C=O)-N<u>H</u>), 10.2 (s, 1H, CH2-N<u>H</u>-(C=O)-NH), 5.8 (s, 1H,

C<u>H</u>=C-CH), 3.3 (m, 4H, NH-(C=O)-NH-C<u>H</u>$_2$ and C<u>H</u>$_2$-NCO), 2.2 (s, 3H, C<u>H</u>$_3$-C=CH$_2$), 1.6 (m, 4H, N-C<u>H</u>$_2$-C<u>H</u>$_2$) and 1.4 (m, 4H, CH$_2$-CH$_2$-C<u>H</u>$_2$-CH$_2$-CH$_2$) ppm. FT-IR ν: 1675, 1701, 2279, 3233, 3466 cm.

Figure 9: Synthesis of UPy-functionalized isocyanate (UPy-NCO).

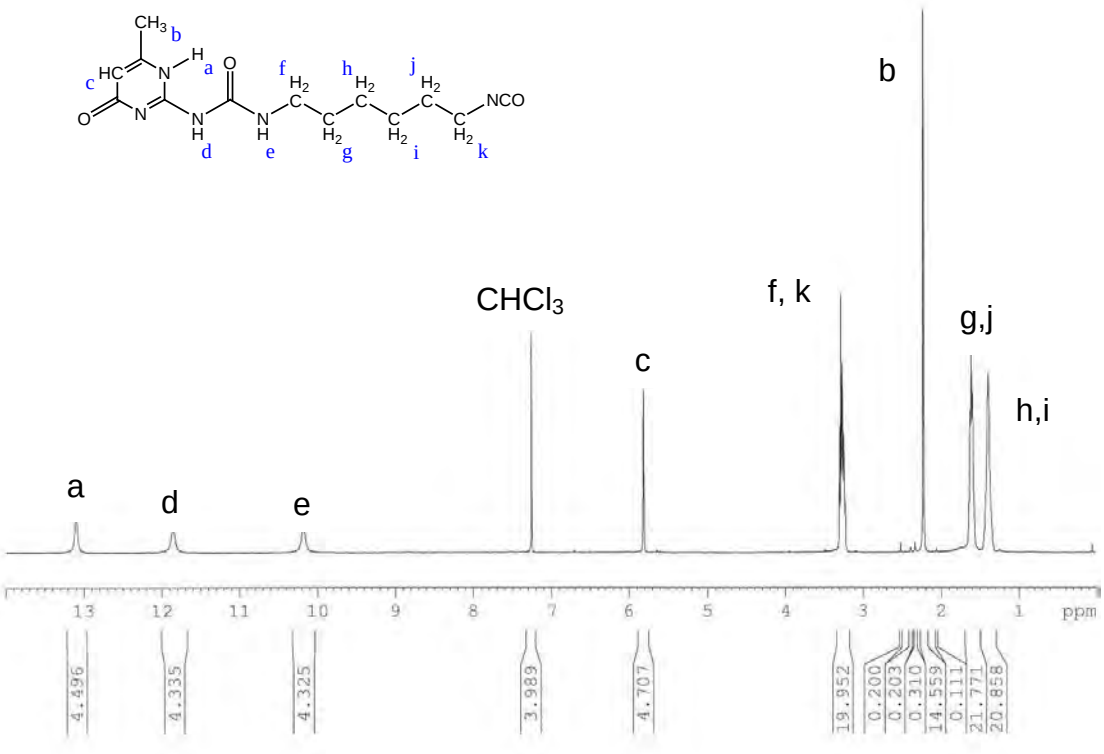

Figure 10: ^{1}H NMR (CDCl$_3$, 400 MHz) of synthesized UPy-isocyanate.

3.1.2 Synthesis of UPy-PEO-UPy

Following the reaction scheme shown in Figure 11, 0.720 g polyethylene glycol (PEG, 2,000 g/mol) was dissolved in 12.0 mL chloroform (dried over molecular sieves). 0.410 g UPy-isocyanate (1.4 mmol) and 1 drop of dibutyltin dilaurate (DBTDL) were then added, and the solution was stirred for 16 hours at 60 °C, under N_2 purge. An additional 12.0 mL $CHCl_3$ was added, and the mixture was filtered under an N_2 blanket. The filtrate volume was then reduced to 12 mL under vacuum, 0.117 g silica gel and 1 drop DBTDL were added, and the reaction allowed to proceed for an additional hour at 60 °C. The silica gel was removed by filtration, and the solvent removed under vacuum. The resulting white waxy solid was dried completely in 50 °C vacuum oven overnight. ^1H NMR ($CDCl_3$, 400MHz) was collected to confirm attachment of UPy groups (Figure 12). Given the broadness of the UPy peaks and the relative, large intensity of the peak corresponding to the PEO backbone, quantitatively confirming functionalization of both ends of the polymer was not feasible.

Figure 11: Synthesis of telechelic UPy-PEO-UPy from hydroxyl-terminated PEO.

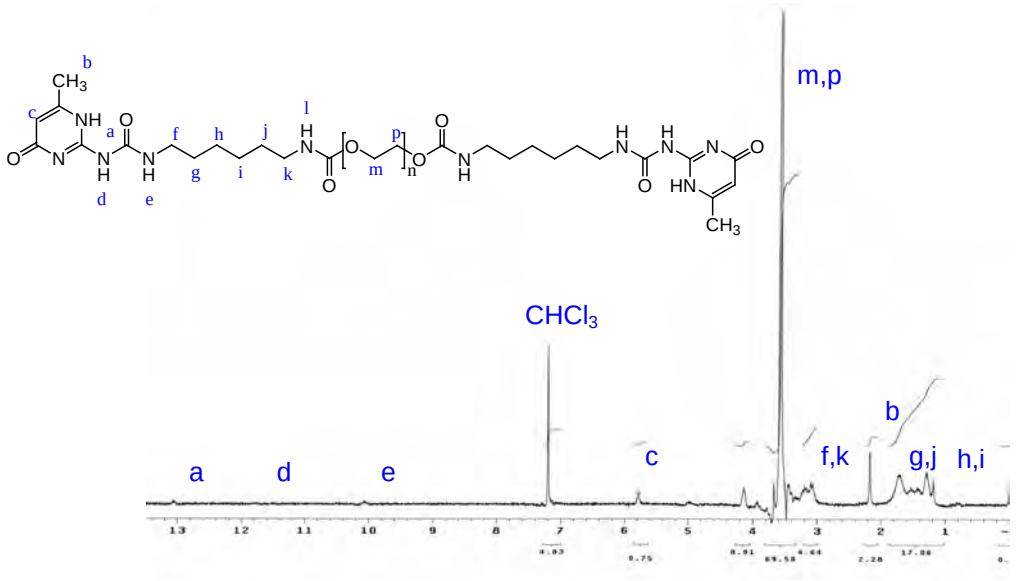

Figure 12: ^{1}H NMR ($CDCl_3$, 400MHz) of telechelic UPy-PEO-UPy.

Matrix-assisted laser desorption/ionization time of flight mass spectrometry (MALDI-ToF) is used in the detection and characterization of polymers and biomolecules. MALDI-ToF spectra were collected for the prepared UPy-PEO-UPy and the unfunctionalized PEG starting material (both shown in Figure 13) to check for complete functionalization of the end-groups. MALDI-ToF is a powerful technique in which a light absorbing matrix is mixed with the sample of interest. This mix of matrix and sample is then irradiated with a laser pulse which ionizes the sample. The ions are accelerated in an electric field, and different molecules are separated according to their mass-to-charge ratio. Since the time it takes for each molecule to reach the detector varies, a separate signal is obtained for each molecule. MALDI-ToF is used for detection and characterization of polymers and

biomolecules. The MALDI-ToF spectrum of the synthesized UPy-PEO-UPy revealed the presence of telechelic UPy-functionalized PEO (boxes in Figure 13), monofunctional PEO and numerous side products which are shown in Figure 14.

Many of the observed side products were attributed to the presence of water in the reaction system. Polyethylene glycol has a high affinity for atmospheric water and isocyanates are highly reactive with water. In addition, residual diisocyanate in the UPy-NCO likely contributed to the formation of side products. In light of the MALDI-ToF data, it was concluded that the complete removal of water from the reaction, and the absence of any residual, unreacted diisocyanate, are paramount to the successful preparation of telechelic UPy-functionalized polymers with minimal side products.

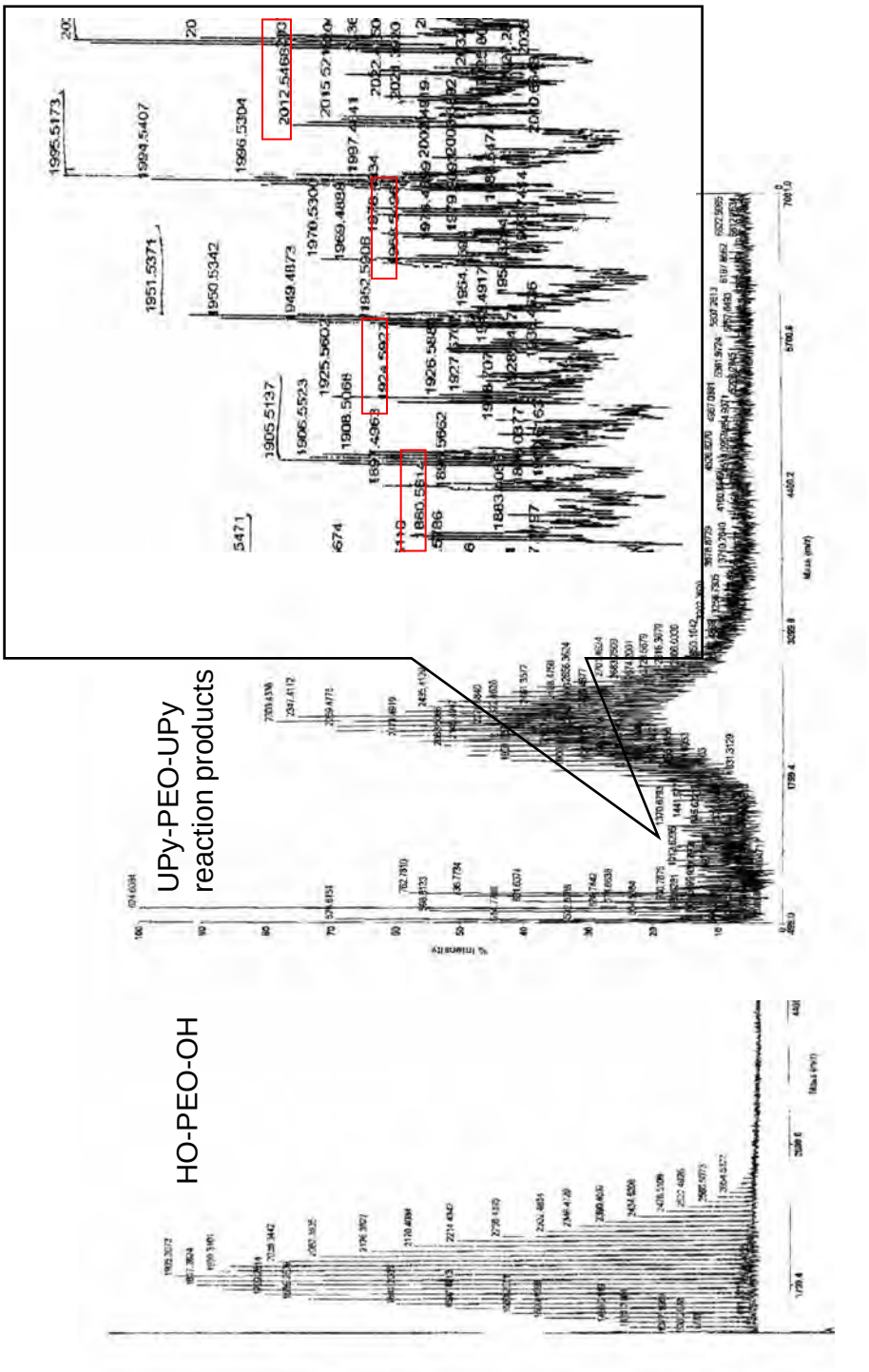

Figure 13: MALDI-ToF spectra of PEO (left) and telechelic UPy-PEO-UPy (right). Boxes indicate peaks corresponding to targeted UPy-PEO-UPy product.

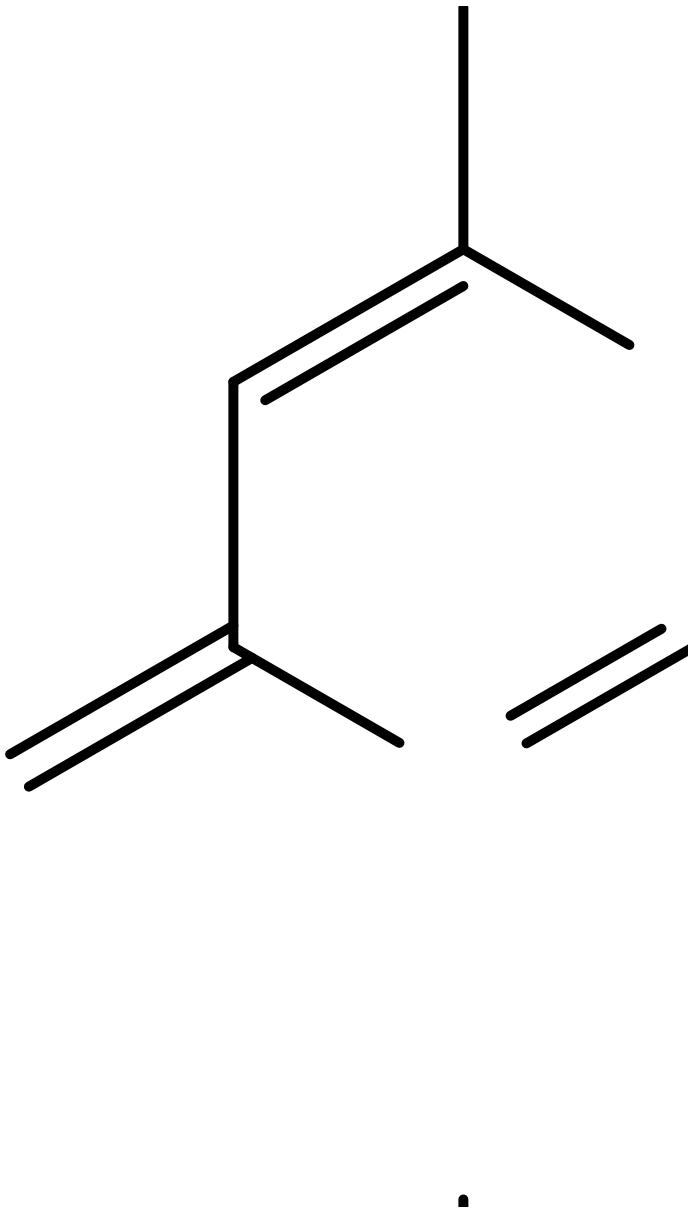

Figure 14: Structure of compounds present in MALDI-ToF spectra of UPy-PEO-UPy shown in Figure 13.

3.1.3 Synthesis of UPy-PB-UPy

1.10 mL (0.35 mmol) hydroxyl-terminated polybutadiene (2,800 g/mol, PDI = 2.21) was dissolved in 12.0 mL chloroform (dried over molecular sieves). 0.412 g UPy-isocyanate (1.4 mmol) and 1 drop of dibutyltin dilaurate (DBTDL) were then added, and the solution was stirred for 16 hours at 60 °C, under N_2 purge. An additional 12.0 mL $CHCl_3$ was added, the resulting mixture centrifuged, and the supernatant removed by pipette. The supernatant volume was reduced to 12 mL under vacuum, 0.119 g silica gel and 1 drop DBTDL were added, and the reaction allowed to proceed for an additional hour at 60 °C. The silica gel was removed by filtration, and the solvent was removed under vacuum. The resulting light yellow, waxy solid was dried completely in 60 °C vacuum oven overnight. ^{1}H NMR ($CDCl_3$, 400MHz) was collected to confirm attachment of UPy groups (Figure 15).

All of the expected peaks corresponding to the UPy end-groups (peaks a-e in Figure 15) were observed. However, concluding that all of the hydroxyl ends of the polybutadiene were converted to UPy groups was not possible. The polydispersity of the polybutadiene starting material (PDI=2.21) precludes confirmation of full functionalization by NMR. Comparison of the integration of NMR peaks corresponding to the CH=CH hydrogens on the polybutadiene backbone with those of the peaks corresponding to the UPy group shows that the 45-100% of the hydroxyl end-groups have been successfully converted to the ureidopyrimidinone functionality.

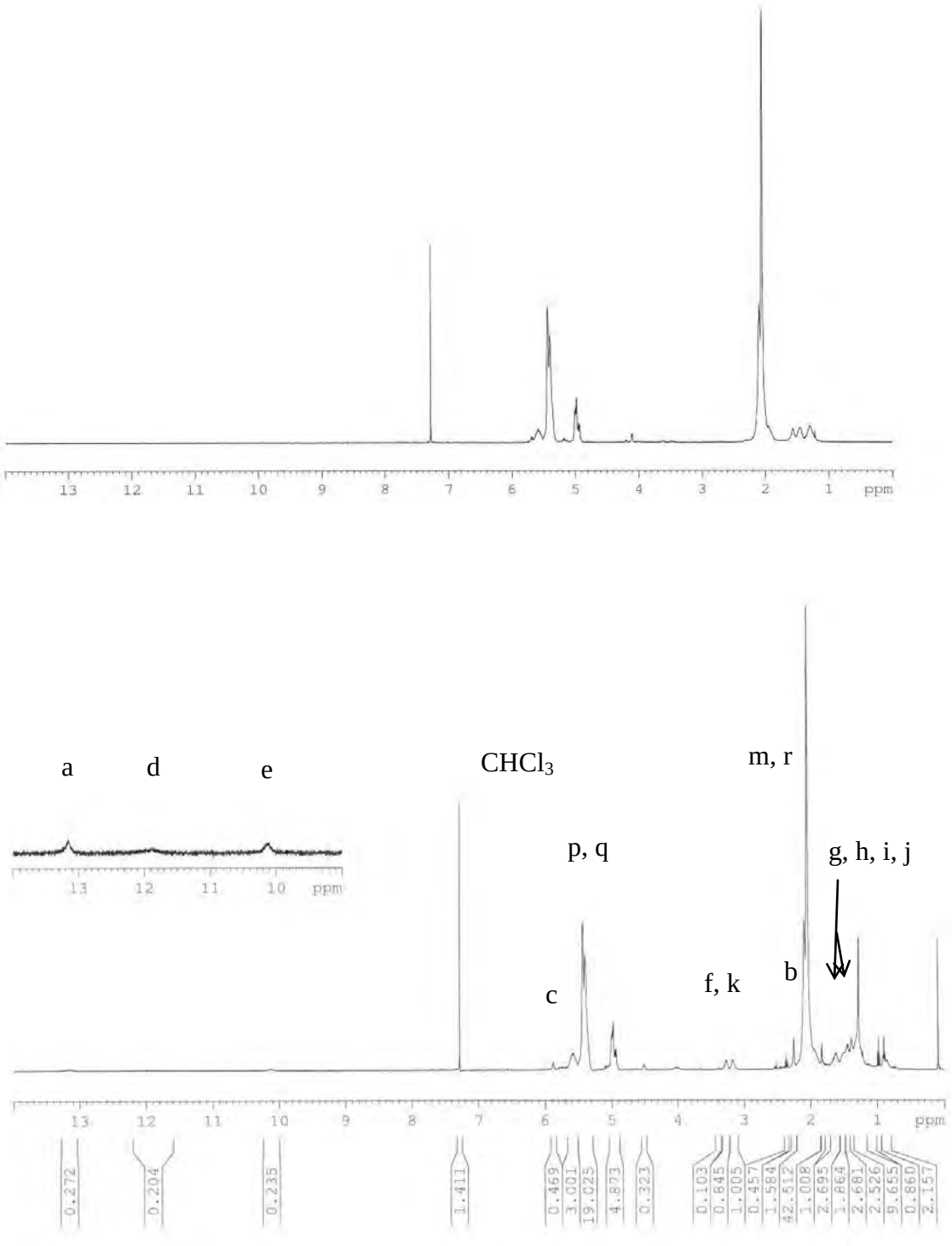

Figure 15: ^{1}H NMR spectra (400MHz, $CDCl_3$) of hydroxyl-terminated polybutadiene before (top) and after (bottom) UPy-functionalization.

3.2 Synthesis of telechelic UPy-functionalized polymers via imidazole chemistry

Meijer's group has reported the synthesis of telechelic UPy materials through the use of oligomers with terminal amino groups.[66] This approach offers advantages over the isocyanate chemistry detailed in the previous section. The UPy-imidazole is less sensitive to humidity than the UPy-isocyanate and the carbonyldiimidazole starting material is significantly less toxic than the HDI. A UPy-functionalized imidazole was prepared that could then be reacted with the amine end-groups of the target oligomers. The addition of a second route to incorporate UPy end-groups onto a polymer increases the number of commercially available polymers that can be used to prepare UPy end-functionalized polymers.

3.2.1 Synthesis of UPy-functionalized imidazole (UPy-imidazole)

Figure 16 shows the synthetic route used to prepare ureidopyrimidinone functionalized imidazole. The reaction details are as follows: in a dried 100 mL round bottom flask, 0.631 g 2-AHMP, 1.29 g carbonyldiimidazole (CDI) were dissolved in 10.0 mL DMSO. The solution was stirred at 60 °C for 2 hours under N_2 purge. The reaction flask was removed from the oil bath and allowed to cool. The product was isolated by precipitation with 10.0 mL acetone followed by filtration, and additional acetone washes. The recovered product, 2-(1-imidazolylcarbonylamine)-6-methyl-4[1H]-pyrimidinone, (UPy-imidazole) was dried in a 40 °C vacuum oven

overnight. An FT-IR spectrum was collected to confirm formation of the UPy-imidazole product. The FT-IR spectrum for our product agrees with that reported in the literature[66] showing peaks at ν = 3173, 3084, 2545, 1698, 1641, 1598, 1506, 1470, 1372, 1318, 1275, 1232, 1190, 1168, 1089, 1063, 1026, 982, 930, 912, and 852 cm^{-1}. There was no evidence of the presence of any residual starting materials.

Figure 16: Synthesis of UPy-imidazole.

3.2.2 Synthesis of UPy-PDMS-UPy via imidazole chemistry

A telechelic, UPy-functionalized PDMS was synthesized following the reaction scheme shown in Figure 17. To ensure functionalization of both terminal ends of the polymer, an excess of UPy-imidazole was employed. In a reaction flask, 0.1791g UPy-imidazole (0.8 mmol) and 0.50 mL amine-terminated poly (dimethyl

siloxane) (0.2mmol, 2335 g/mol, Aldrich) were dissolved in 10.0 mL chloroform (dried over molecular sieves). The reaction was allowed to run overnight (18 hours) at 65 °C, under N_2 purge. The solvent was removed under vacuum and the resulting polymer was characterized by FT-IR (Figure 18). The appearance of peaks at ν = 1698, 1668 and 1598 cm^{-1} confirm the attachment of UPy groups.[66]

Figure 17: Synthesis of UPy-PDMS-UPy via imidazole chemistry.

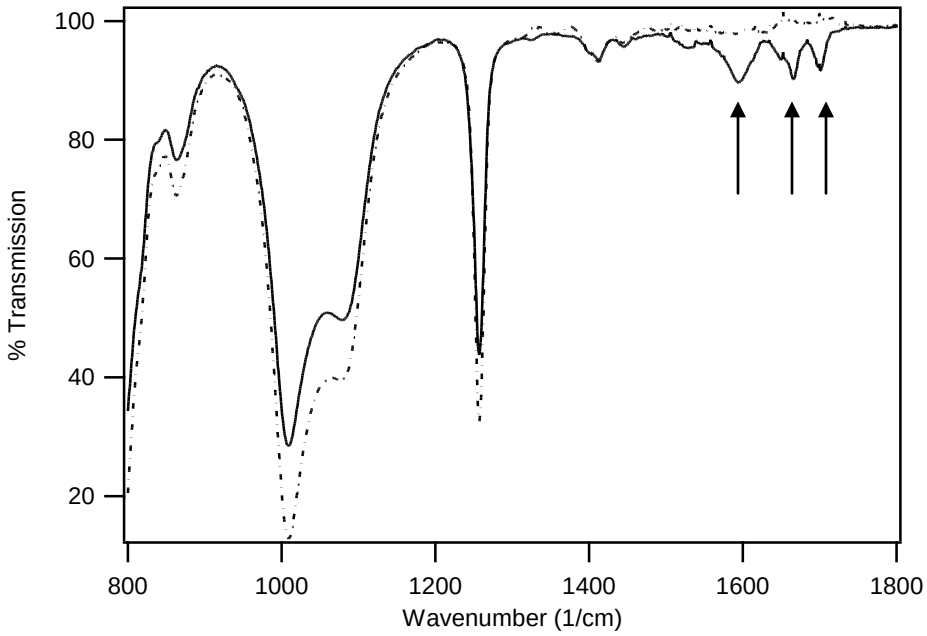

Figure 18: FT-IR of H_2N-PDMS-NH_2 (dashed line) and UPy-PDMS-UPy (solid line) showing incorporation of UPy end-groups. Arrows indicate peaks corresponding to the incorporated UPy functionalities.

3.3 ATRP/ATRC approach to well defined, UPy-functionalized polymers

The functionalization of commercially available oligomers discussed in the previous sections was somewhat limiting in that there was little molecular weight control. Additionally, oligomers with only one end functionalized were not readily available, making the synthesis of pure monofunctional polymers inconvenient.

Atom transfer radical polymerization is a controlled living radical polymerization method that can be used to prepare polymers of controlled molecular weight and low polydispersity. A schematic representation of the mechanism of ATRP is shown in Figure 19. ATRP reactions utilize a metal halide (CuBr here) that forms a complex

with a ligand (L) to form the reaction catalyst. Free radicals are generated by oxidation of the metal/ligand complex and reduction of the initiator (R), typically an alkyl halide. The activated initiator radical can then react with free monomer to form polymer chains, or recombine with the halide resulting in the deactivitation of the reactive radical. A growing polymer chain (R-M• in Figure 19) can then continue to propagate through the addition of monomer, be deactivated by recombination with the halide or terminate by coupling to form a telechelic polymer or by disproportionation.

Control of reaction rate is dependent on control of the rates of activation (k_a), deactivation (k_d), propagation (k_p) and termination (k_t). Careful selection of metal/ligand pairs is crucial to successful control in ATRP reactions. The ligand strongly affects the solubility of the metal complex as well as the dynamics of the reaction equilibrium. In addition, a small amount of the corresponding divalent metal halide (copper(II)bromide in this work) can be added to increase control of the reaction rate by encouraging deactivation and limiting the number of free radicals in the reaction mixture.

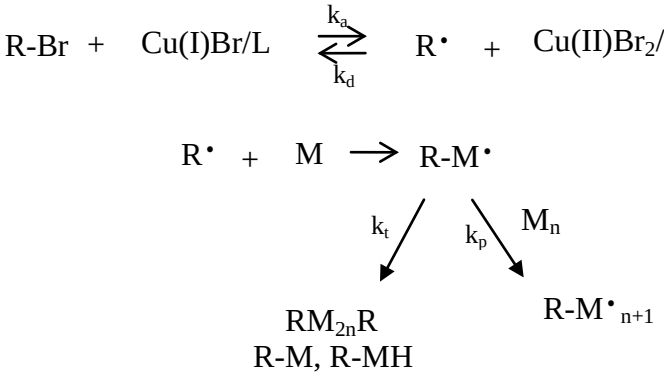

Figure 19: Mechanism of ATRP polymerization.

The use of functionalized initiators for ATRP provides a route to the synthesis of end-functionalized polymers. ATRP with a hydroxyl functional initiator to yield monofunctional hydroxyl terminated polymers has been reported in the literature.[67] These polymers were then coupled by ATRC to yield telechelic hydroxyl-terminated polymers of controlled molecular weight. The ATRP/ATRC reaction scheme used in this work is shown in Figure 20.

Figure 20: Synthesis of monofunctional and telechelic hydroxyl-functionalized PS by ATRP/ATRC.

Copper (I) bromide forms a coordination complex with the PMDETA amine and acts as a catalyst for the polymerization. A small amount of copper (II) bromide is used to control the rate of reaction and limits the concentration of active radicals. A low active polymer radical concentration minimizes the number of growing polymer chains that terminate through radical coupling and disproportionation,

affording lower polydispersity. Molecular weight control was achieved by varying the concentration of the initiator and catalyst complex, and by varying the reaction time.[87] The mono-functional, bromine-terminated polymer prepared by ATRP then acts as an initiator for the coupling reaction (ATRC). In this second step, a small amount of zero-valent copper metal is used to increase the concentration of radicals, encouraging coupling to form telechelic polymers.

3.3.1 Synthesis of 2-hydroxyethyl-2-bromoisobutyrate initiator (HEBrIBu)

The synthetic scheme used to prepare the hydroxyl-terminated initiator is shown in Figure 21. The following were added to a dried round bottom flask: 4.66 g ethylene glycol, 10.35 g N, N-dicyclohexylcarbodiimide (DCC), 8.37 g 2-bromo-2-methylpropionic acid (BMP) and 50.0 mL dichloromethane (DCM). The resulting suspension was cooled in an ice bath and 63.4 mg dimethylaminopyridine (DMAP) was added with stirring. After an additional 5 minutes, the reaction flask was removed from ice bath and allowed to warm to room temperature. The reaction was allowed to proceed, with stirring, overnight. Dicylcohexyl urea precipitate formed over the course of the reaction. An additional 50.0 mL DCM was added with stirring and the reaction mixture was filtered. The solids were washed twice with an additional 25 mL DCM. The solvent was removed from the resulting filtrate under vacuum. The product, a slightly yellow, viscous liquid was purified by gradient column chromatography using 4/1 to 2/3 hexane/ether. After vacuum drying

overnight at 25 °C, ^{1}H NMR (Figure 22) was used to confirm formation of desired product. ^{1}H NMR (400 MHz, $CDCl_3$): δ = 4.31(t, 2H, $OC\underline{H_2}CH_2OH$), 3.86 (t, 2H, $OCH_2C\underline{H_2}OH$), 1.95 (s, 6H, $C(Br)C\underline{H_3}$).

Figure 21: Synthesis of 2-hydroxyethyl-2-bromoisobutyrate (HEBrIBu) initiator for ATRP/ATRC.

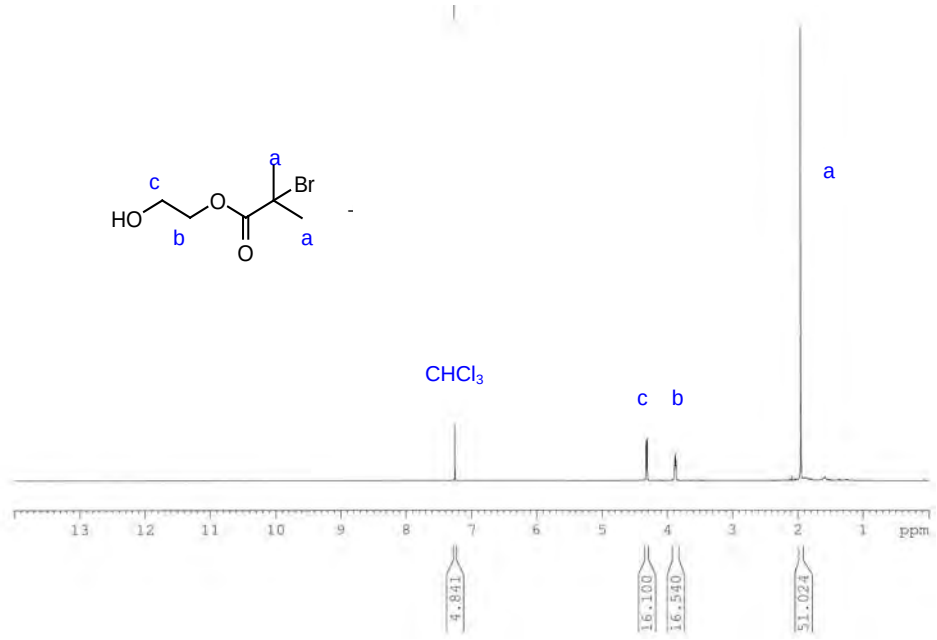

Figure 22: ^{1}H NMR of 2-hydroxyethyl-2-bromoisobutyrate initiator (HEBrIBu).

3.3.2 ATRP of monofunctional hydroxyl-terminated polystyrenes (HO-PS-Br)

Material purifications:

The styrene monomer was stirred over calcium hydride overnight, distilled, and bubbled with N_2 for 30 minutes immediately prior to use. The copper (II) bromide was washed with glacial acetic acid, followed by isopropanol. The copper (II) bromide and copper (I) bromide were dried in a vacuum oven prior to use. All other materials were used as received.

Synthesis:

The following were added to a 100 mL airfree flask: 254 mg copper (I) bromide, 21 mg copper (II) bromide and a stir bar. Flask was degassed and backfilled with N_2 three times. Styrene (10.0 mL) and N,N,N',N",N"-pentamethyldiethylene triamine (PMDETA) (0.40 mL) were added using dried syringes. The reaction solution was stirred until a color change to bright green indicated complex had formed. Three freeze-dry-thaw cycles were performed prior to the addition of 495 mg HEBrIBu initiator. The flask was immersed in an 85 °C oil bath for the 2 hour reaction. The flask was then removed from the oil bath, and the reaction was stopped by exposure to air and the addition of 5.0 mL tetrahydrofuran (THF). The residual copper was removed by passing through an alumina column. The product was then precipitated in methanol. After filtration, the solid product was dried in a 60 °C vacuum oven. The product was characterized by gel permeation chromatography (Figure 23) to give M_n = 1,530 g/mol and PDI = 1.27.

3.3.3 ATRC preparation of telechelic hydroxyl-terminated polystyrenes (HO-PS-OH)

Material purifications:

Copper (II) bromide was washed with glacial acetic acid, followed by isopropanol, and dried in a vacuum oven prior to use. Toluene was distilled (discarded first fraction) and bubbled with N_2 30 minutes immediately prior to use. All other materials were used as received.

Synthesis:

The following were added to a 100 mL airfree flask: 56.5 mg copper (I) bromide, 0.902 g HO-PS-Br (M_n = 1,530 g/mol) and a stir bar. The flask was degassed and backfilled the N_2 three times. 10.0 mL toluene was added and the reaction mixture stirred to dissolve the polymer. 0.150 mL N,N,N',N",N"-pentamethyldiethylene triamine (PMDETA) was added using dried syringe. The solution was stirred until a color change indicated the complex had formed. Three freeze-dry-thaw cycles were carried out and 96 mg nano-copper powder was added under positive N_2 flow. The reaction flask was immersed in 80 °C oil bath for four hours. The reaction was quenched by exposure to air and the addition of 10.0 mL THF. The residual copper was removed by passing through an alumina column. The product was then precipitated into methanol, filtered and dried under vacuum at 60 °C. The product was characterized by GPC. A summary of all the hydroxyl-terminated polymers prepared using ATRP/ATRC with HEBrIBu is shown in Table 2. Figure 23 shows example GPC chromatograms of a synthesized telechelic hydroxyl-terminated polystyrene and its monofunctional precursor. The telechelic

material has a number-averaged molecular weight of 3,060 g/mol and PDI = 1.34. There is approximately 19% unreacted monofunctional polystyrene remaining for the sample shown.

Table 2: Summary of ATRP/ATRC reactions using HEBrIBu initiator.

CuBr (mmol)	$CuBr_2$ (mmol)	nano-Cu (mmol)	Styrene (mmol)	PMDETA (mmol)	Initiator (mmol)	Temp (°C)	time	M_n [a] (g/mol)	PDI[a]
1.78	0.11	--	87	1.91	0.74	85	2 hr	7,978	1.06
0.40	--	1.45	--	0.72	0.11	80	2 hr	13,236	1.12
1.78	0.094	--	87	1.91	0.98	85	2 hr	1,530	1.27
0.40	--	1.50	--	0.72	0.61	82	2 hr	3,060	1.34
0.53	0.03	--	87	0.53	0.23	85	2 hr	62,972	1.39

Shaded rows indicate ATRC coupling reactions.
a) Determined by GPC analysis.

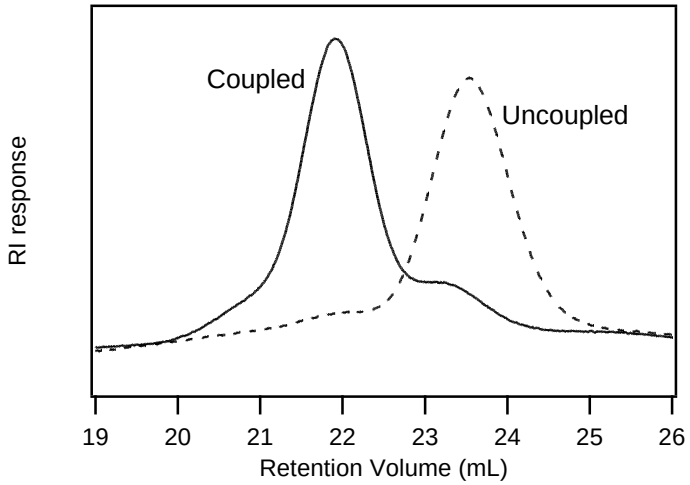

Figure 23: GPC chromatogram of monofunctional and telechelic hydroxyl-terminated polystyrenes.

3.3.4 UPy-functionalization of HO-PS-OH

211 mg HO-PS-OH (3,060 g/mol) was dissolved in 10.0 mL chloroform (dried over molecular sieves). One drop dibutyltin dilaurate and 165 mg UPy-isocyanate were added. The reaction proceeded 16 hours at 60 °C under N_2 purge. After reaction, an additional 10.0 mL $CHCl_3$ was added and the mixture was filtered. Silica gel (52 mg) and one drop of dibutyltin dilaurate were added to the filtrate. The mixture was allowed to react one additional hour at 60 °C and was subsequently filtered to remove the silica gel. The solvent was then removed from the filtrate under vacuum. The resulting solid product was dried in a 60 °C vacuum oven. The product obtained was a waxy orange solid with a molecular weight of approximately 3,600 g/mol based on the molecular weight of the hydroxyl-terminated precursor. Due to large number of hydrogen atoms in the polystyrene backbone, the hydrogen atoms of the UPy groups were not able to be observed with ^1H NMR. A high conversion of hydroxyl groups to UPy groups was concluded based upon the disappearance of the terminal hydroxyl peaks (Figure 24).

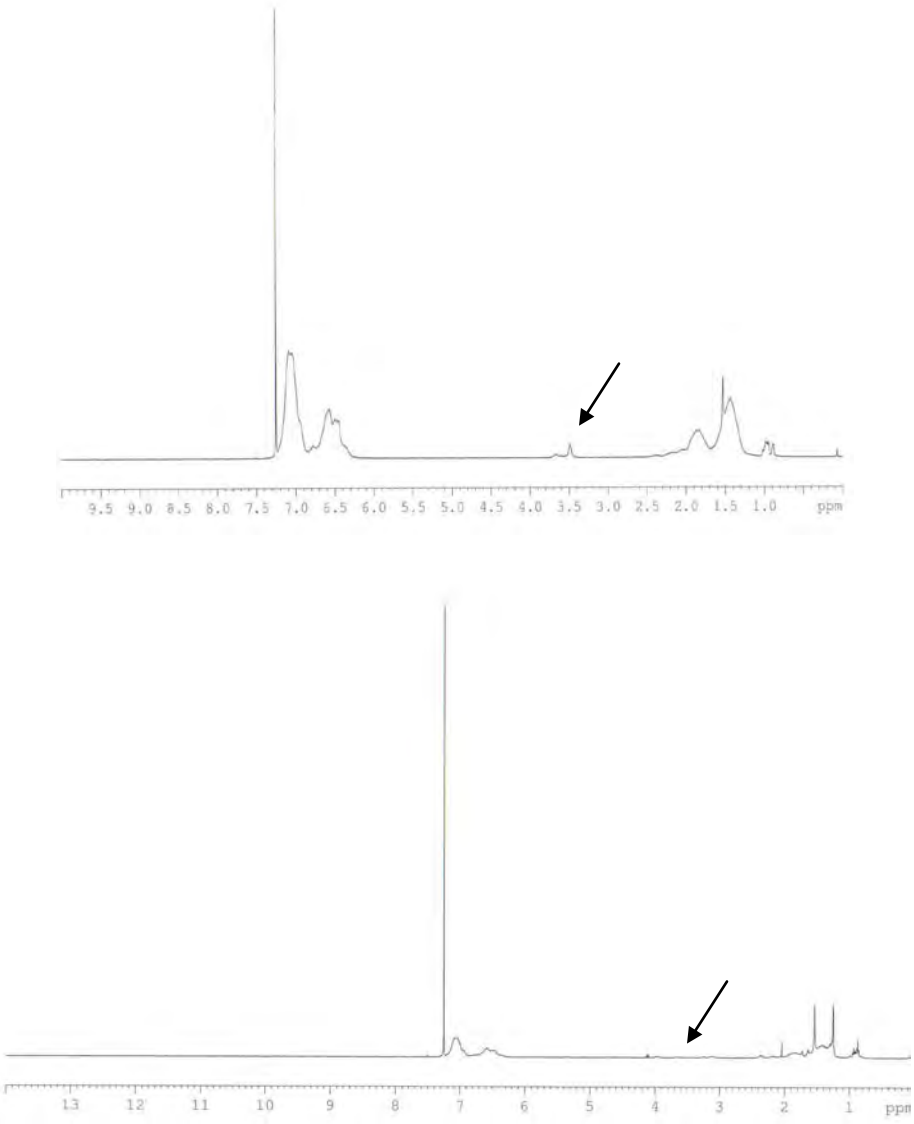

Figure 24: ^{1}H NMR (400MHz, $CDCl_3$) spectra of hydroxyl-terminated polystyrene before (top) and after (bottom) UPy functionalization. Peak at 3.5 ppm (arrows) corresponding to hydroxyl groups disappears after UPy-functionalization indicating complete conversion of terminal OH groups to terminal UPy groups.

3.4 Synthesis of UPy-terminated polymers using a UPy-functionalized ATRP initiator

In polymerization reactions, the use of functionalized initiators ensures the formation of functional polymers. Building upon the success in synthesizing hydroxyl- terminal polymers from HEBrIBu, a UPy-functionalized initiator was prepared and used in atom transfer radical polymerization (ATRP). This section details the results of synthetic runs to prepare UPy-functionalized polymers. The reaction scheme for polystyrene is illustrated in Figure 25. One example of each polymer synthesis reaction will be discussed below. Several additional runs were performed to achieve different molecular weights by varying the concentration of the initiator and catalyst complex and by varying the reaction time.

3.4.1 Synthesis of UPy-functionalized bromoisobutyrate initiator

Following the reaction scheme shown Figure 26, 1.51 g (7.11 mmol) HEBrIBu was dissolved in 100 mL chloroform (dried over molecular sieves). 4.20 g (14.1 mmol) UPy-NCO and 1 drop of dibutyltin dilaurate (DBTDL) were then added, and the solution was stirred for 16 hours at 60 °C, under N_2 purge. An additional 50 mL $CHCl_3$ was added, and the mixture was filtered under an N_2 blanket. The filtrate volume was then reduced to 100 mL under vacuum, 1.18 g silica gel and 1 drop DBTDL was added, and the reaction allowed to proceed for an additional hour at 60 °C. The silica gel was removed by filtration, and the solvent removed under vacuum.

Figure 25: Scheme showing ATRP/ATRC of styrene using a UPy-functionalized bromoisobutyrate initiator to form monofunctional (M-PS) and telechelic (T-PS) UPy-polymers.

The resulting white powder was dried completely in a 50 °C vacuum oven overnight. ^{1}H NMR spectroscopy, shown in Figure 27, was used to confirm complete UPy functionalization of the 2-hydroxyethyl-2-bromoisobutyrate initiator starting material. The peaks at δ = 13.1, 11.9, and 10.2 ppm correspond to single hydrogens on the UPy group. The peaks at 4.3 ppm correspond to the CH_2 groups between the oxygen atoms of the hydroxyl terminated initiator. The 1:4 ratio of the peak integrations shows that all of the initiator chains have UPy terminals in place of the original hydroxyl group. The complete assignment of peaks is as follows: (400mHz, $CDCl_3$):

δ = 13.1 (s, 1H, $CH_3CN\underline{H}$), 11.9 (s, 1H, $CH_2NH(C=O)N\underline{H}$), 10.2 (s, 1H, $CH_2N\underline{H}(C=O)NH$), 5.8 (s, 1H, $C\underline{H}=CCH_3$) 4.31(t, 2H, $OC\underline{H_2}CH_2OH$), 3.2 (t, 4H, $NH(C=O)NHC\underline{H_2}$ + $C\underline{H_2}NCO$), 2.2 (s, 3H $C\underline{H_3}C=CH$), 1.95 (s, 6H, $C(Br)C\underline{H_3}$), 1.6 (m, 4H, $NCH_2C\underline{H_2}$), 1.4 (m, 4H, $CH_2CH_2\underline{CH_2}CH_2CH_2$).

Figure 26: Synthesis of UPy-functionalized bromoisobutyrate initiator (UPy-BrIBu).

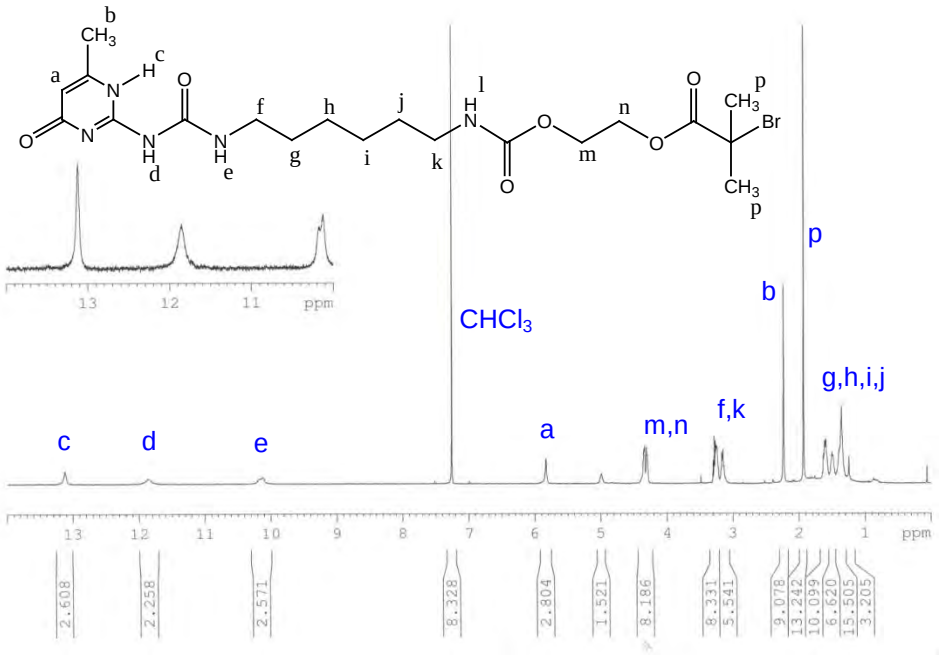

Figure 27: NMR of synthesized UPy-bromoisobutyrate initiator (UPy-BrIBu).

3.4.2 ATRP with UPy-functionalized bromoisobutyrate initiator (UPy-BrIBu)

Material purifications:

The CuBr was washed with glacial acetic acid, followed by isopropanol. The washed CuBr, $CuBr_2$, and UPy-functionalized initiator were dried at 60°C in a vacuum oven overnight immediately before use. The 1,6-hexane diisocyanate, styrene, methyl methacrylate, and PMDETA were each distilled before use. All liquid reagents used in ATRP/ATRC procedures were bubbled with nitrogen gas for at least 30 minutes immediately before use. All other materials were used as-received.

Synthesis:

ATRP and ATRC were performed in a similar manner as that described in section 3.3.2 and 3.3.3, respectively, taking into consideration the increased molecular weight of the UPy-functionalized bromoisobutyrate initiator when determining the amount of material to use. Reaction times and molar ratios were varied in attempt to synthesize different molecular weight polymers. Polystyrene, poly(methyl methacrylate) and poly(4-methylstyrene) were successfully prepared by this method.

Following the ATRP reactions, proton NMR was used to verify the presence of UPy end-groups (δ = 13.1, 11.9, 10.2 ppm), but could not be used to quantitatively confirm functionalization due to saturation of the NMR signal by the hydrogens of the polymer backbones. For higher molecular weight materials, the peaks

corresponding to the hydrogens on the UPy end-group could not be detected by ^{1}H NMR. Successful functionalization of the prepared polymers was assumed based on the confirmed functionality of the initiator (section 3.4.1). Details of the ratios of reactants used and reaction conditions are listed in Appendix A.

The molecular weight characteristics of all the mono-functional and telechelic UPy-functionalized polymers synthesized by ATRP/ATRC are summarized in Table 3. Given the large number of samples to be discussed, abbreviated sample names were assigned. Sample names were chosen to provide the following information: architecture ("M" for mono-functional or "T" for telechelic), backbone type (ex., "PS" or "PMMA"), and molecular weight (in kDa). Compared with ATRP reactions of styrene using 2-hydroxyethyl 2-bromoisobutyrate, the use of UPy-functionalized initiators resulted in similar reaction kinetics, but larger polydispersities (except for M-PS-6**)**. However, MMA reaction rates were considerably higher than those reported in the literature. Our ATRP process resulted in PMMA molecular weights at least double those reported by Sarbu *et al*. under similar conditions with identical reaction times (Table 4).[67] In addition, the polydispersities for ATRP with MMA were even higher than those for styrene. The observed high polydispersities may be due to the increased efficiency of the bulky UPy-functionalized initiator. Increasing the size of the end-group of haloester ATRP initiators has been reported to result in increased efficiency, which can lead to higher polydispersities.[88] A possible approach to improving polydispersities may be to increase the amount of $CuBr_2$ in order to slow the reaction kinetics. GPC results will be discussed in more detail in Chapter 4.

Table 3: Summary of characteristics of selected UPy-functionalized polymers prepared by ATRP/ATRC.

Sample	M_n (g/mol)[a]	PDI[a]
M-PS-2	2,300	1.12
T-PS-5	9,700	1.60
M-PS-6	6,000	1.02
T-PS-12	48,900	1.49
M-PS-11	10,700	1.47
T-PS-19	19,000	1.81
M-PS-26	25,600	1.89
M-PMMA-6	6,300	1.65
T-PMMA-13	19,500	2.32
M-PMMA-13	13,200	3.01

a) Determined by GPC.

Table 4: Summary of ATRP/ATRC reactions reported by Sarbu et al.[67]

CuBr (mmol)	$CuBr_2$ (mmol)	nano-Cu (mmol)	Monomer (mmol)	PMDETA (mmol)	Initiator (mmol)	Temp (°C)	time	M_n (g/mol)	PDI
1.75	0.087	--	S-87	1.83	1.75	80	2 hr	2,550	1.08
0.36	--	1.46	--	0.73	0.36	70	4 hr	4,910	1.21
1.75	0.087	--	MMA-87	1.83	1.75	50	2 hr	1,880	1.05
0.96	--	3.83	S-0.96	1.92	0.96	70	5 hr	3,560	

3.5 Conclusions

While the functionalization of commercially available telechelic polymers can be used to prepare UPy-functionalized polymers, this approach has several drawbacks. First, selection of polymer backbone and the molecular weight of that backbone are

determined by commercial availability. Second, purification of telechelic product to remove any monofunctional polymer is cumbersome at best.

The first drawback is easily avoided by first using ATRP/ATRC to prepare polymers of controlled molecular weight and polydispersity having end-groups that can alter be converted to ureidopyrimidinone functionalities. In fact, ATRP allows the creation of well-defined monofunctional polymers as well. However, the same difficulties in purification of telechelic UPy-functionalized polymers remain.

The incorporation of functional groups onto ATRP initiators provides an effective route to the preparation of end-functionalized polymers. Purification of the UPy-BrIBu is straightforward and the polymers synthesized from the functionalized initiator are guaranteed to carry the desired UPy end-group. The attachment of ureidopyrimidinone groups onto 2-hydroxyethyl-2-bromoisobutyrate appears to increase the efficiency of the initiator, resulting in faster reaction rates and greater polydispersities than reported in the literature for other bromoisobutyrate initiators. Additional control of reaction kinetics may be accomplished by increasing the concentration of copper (II) bromide.

Chapter Four: Characterization of UPy-functionalized Polymers

Gel Permeation Chromatography and Differential Scanning Calorimetry were used to characterize the synthesized UPy-functionalized polymers. A brief discussion of each technique, along with results obtained will be presented here.

4.1 Gel Permeation Chromatography

Gel permeation chromatography is a tool often used in the characterization of polymeric materials. Gel permeation chromatography was used to measure the molecular weight and polydispersity of UPy-functionalized polymers synthesized by ATRP/ATRC. The coupling efficiency of a given ATRC synthesis run can also be determined from the GPC chromatogram of the product. Coupling efficiency is particularly relevant to the study of telechelic associating materials in that any residual monofunctional polymers can act as "chain stoppers" and decrease the average number of polymers in an associated chain.[22, 89]

GPC analysis can also reveal the presence of aggregate structures.[90] The aggregation of UPy end-groups into stacks through hydrogen bonding of the adjacent urethane linkage has been previously reported.[48] The formation of aggregate structures, beyond end-to-end association, can have a large effect on the miscibility of polymer blends for several reasons. First, any lateral stacking in addition to end-to-end association will increase the virtual molecular weight of our telechelic samples, decreasing blend miscibility. In addition, while end-to-end association alone should

result in a linear arrangement of polymers, the inclusion of lateral associations that form stacks could result in a branched or network-like structure. Branching or crosslinking to form a polymer network could result in decreased miscibility compared with their linear counterparts.[49, 91]

This section will be organized as follows: a brief description of the instrumentation will be given, followed by a discussion of the calculation of coupling efficiencies from the acquired GPC data. Next, the observation of suspected aggregation and the experiments performed to investigate said aggregation will be discussed.

4.1.1 Instrumentation

GPC instrumentation consisted of an Agilent 1100 HPLC system equipped with a Viscotek triple detector. Three columns were utilized (two Viscotek mixed bed, low M_w, i-series and one mixed bed medium M_w, i-series column). The system temperature was maintained at 60 °C for NMP eluent and 30 °C for THF eluent. Calibration was performed using a series of polystyrene standards of various molecular weights. GPC traces were interpreted using the instrument software package OmniSEC (Viscotek).

4.1.2 Molecular weights and coupling efficiencies of polymers synthesized by ATRP/ATRC

The coupling efficiencies reported in Table 5 were determined by a non-linear least squares fitting of Gaussian peaks to the GPC traces, followed by peak integration. The ratio of the area under the peak(s) corresponding to coupled material to the total area under the curve is reported as the coupling efficiency. Coupling efficiencies were higher for the polystyrene samples than for the poly(methyl methacrylate) samples.

Table 5: Characteristics of select synthesized UPy-terminated polymers.

Sample	M_n (g/mol)[a]	PDI[a]	Monomer Conversion	Coupling Efficiency[a]
T-PS-3[b]	12,100	1.95	-	0.81
M-PS-2	2,300	1.12	17 %	-
T-PS-5	9,700	1.60	-	0.92
M-PS-6	6,000	1.02	30 %	-
T-PS-12	48,900	1.48		0.91
M-PS-11	10,700	1.47	38%	-
T-PS-19	19,000	1.81	-	0.99
M-PS-26	25,600	1.89	15%	-
M-PMMA-6	6,300	1.65	17%	-
T-PMMA-13	19,500	2.32.	-	0.66
M-PMMA-13	13,200	3.01	30%	-

a) Determined by GPC.
b) This sample was prepared by UPy functionalization of ATRP prepared HO-PS-OH with M_n = 3,060 g/mol and PDI = 1.34. Reported coupling efficiency is for synthesis of HO-PS-OH prior to UPy-functionalization.

Acquired GPC data indicate that, following ATRC, telechelic polymers exhibit significantly higher molecular weights than their mono-functional precursors. In theory, ATRC should nearly double the molecular weight. For T-PS-19 this

appears to be nearly true—the ATRC reaction increased molecular mass from 10,700 g/mol to 19,000 g/mol. The corresponding GPC chromatograms for this sample are displayed in Figure 28 and provide convincing evidence that the majority of chains were properly coupled. A minor, high molecular weight shoulder is present in this chromatogram. This shoulder also shifted to higher molecular weight following the ATRC reaction. No other samples exhibited this high molecular weight shoulder, and its origin is unknown.

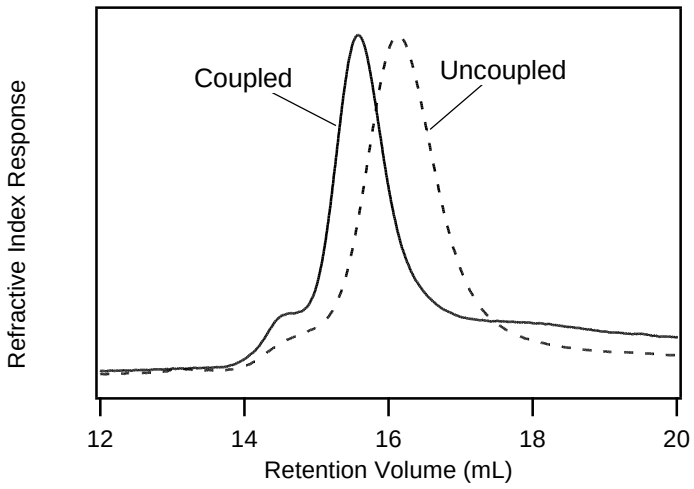

Figure 28: GPC chromatograms for M-PS-11(dashed line) and T-PS-19 (solid line).

GPC analysis of other UPy-functionalized samples following ATRC revealed unexpectedly high molecular weights. In two cases (T-PS-12 and T-PS-3), the chromatograms of coupled polymers showed multiple low retention volume peaks (Figure 29). For these samples, the resulting molecular weights of the coupled products were many times that of the corresponding mono-functional precursors.

Since no free monomer is present in the coupling step of the synthesis, this apparent increase in molecular weight (beyond the near doubling expected for coupling) cannot be due to the growth of the polymer backbone through additional polymerization. Interestingly, the retention volumes of the additional peaks observed by GPC correspond to integer multiples of the expected molecular weight of the prepared polymer suggesting aggregation of the polymer chains.

These low retention volume elution peaks may be due to self-association of hydrogen bonding end-groups, or possibly to aggregation of UPy end-groups into stacks through hydrogen bonding of the urethane linkage.[48] The resulting aggregates must form structures with time-averaged hydrodynamic radii equivalent to higher molecular weight linear coils. The observation of aggregate formation using chromatography techniques such as GPC and HPLC has been previously reported for Bernard's supramolecular H-bonded star polymers[90] and Gong's H-bonding duplexes.[92] For the UPy-containing polymers studied here, the presence of multiple elution peaks was only observed for lower molecular weight samples. These samples contain a higher weight fraction of UPy end-groups, which may explain why they are more susceptible to aggregation.[48]

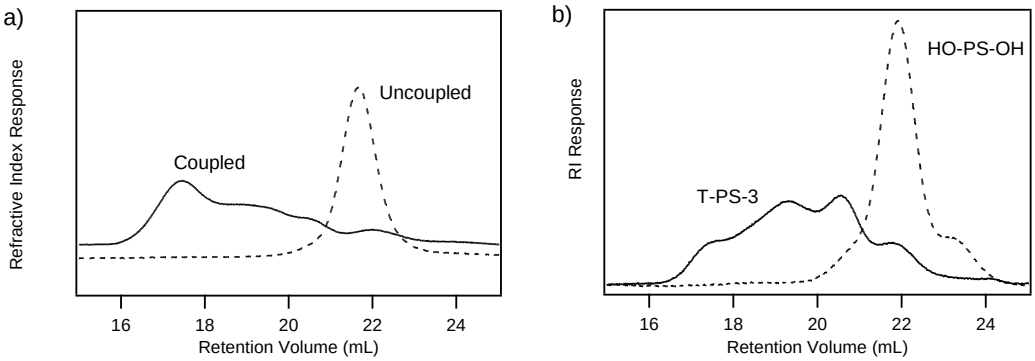

Figure 29: GPC chromatograms of UPy-functionalized polystyrenes showing multiple low retention volume peaks: a) M-PS-6 and T-PS-12 and b) T-PS-3 and HO-PS-OH precursor. Mobile phase was n-methyl pyrollidinone; column temperature was 60 °C.

4.1.3 Investigation of suspected aggregation of UPy end-groups

Two experiments were carried out to further investigate the suspected aggregation of T-PS-12 and T-PS-3 observed with GPC. A small amount of the UPy-NCO was added to a solution of T-PS-12 in THF to intentionally disrupt association into long chains. The resulting chromatogram (Figure 30) showed a slightly greater amount of free polymer and a lower amount of high molecular weight aggregates compared to the sample without the UPy-NCO. This observation is consistent with earlier studies of UPy-terminated polymers which showed that the addition of "chain stopper" decreases intermolecular association.[89, 93] The existence of some aggregation despite the presence of chain stopper indicates that the UPy groups form stable aggregates in solution. This observed aggregate stability may be due the presence of the urethane linkages which can still form stacks in the presence of the UPy-NCO.

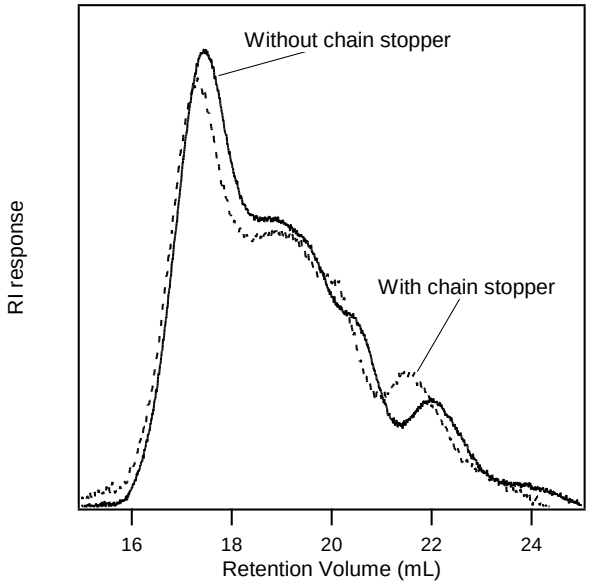

Figure 30: GPC experiments with chain stopper. Chromatograms of 12K UPy-PS-UPy with and without chain stopper present. Mobile phase was n-methyl pyrollidinone; column temperature 60 °C.

Removal of UPy end-groups from PS backbones

In a second experiment, trifluoroacetic acid (TFA) was used to completely remove the associating UPy end-groups by cleavage of the urethane or urea functional groups and a new GPC chromatogram collected. Two samples were tested, M-PS-2 and T-PS-12. Each were dissolved in solutions of THF and trifluoroacetic acid (TFA). After sitting several days at ambient conditions, the THF and TFA were removed under vacuum. The resulting dried samples were then stirred overnight in 0.1M HCl to remove any cleaved UPy end-groups, followed by filtration and vacuum drying. ^{1}H NMR of the TFA washed M-PS-2 sample (Figure 31) indicate the absence of the peaks between 10 and 14 ppm that correspond to UPy protons (δ = 13.1, 11.9, 10.2 ppm), while the PS backbone remains intact. The GPC

chromatogram for the TFA-washed T-PS-12 did not show elution peaks that correspond to molecular weights greater than 12,000 g/mol (Figure 31**).** This confirms that the lower retention volume peaks in Figure 29 are due to end-group aggregation. The observation of aggregation of UPy end-groups by GPC has not previously been reported in the literature.

The GPC chromatogram of the TFA-washed M-PS-2 was unchanged indicating that if the UPy end-groups were associated in the original GPC sample, the associations did not survive the GPC columns and the measured molecular weight was that of unassociated unimers and not dimers. This is in agreement with Long's group[11] who reported that the UPy associations of monofunctional samples were not observed by GPC. Long prepared UPy-PS samples from monofunctional hydroxyl-terminated polymers prepared by living anionic polymerization and characterized the resulting polymers using rheology, DSC and GPC. Long attributed the lack of observed association to the dilute concentration of typical GPC samples (1 mg/mL).

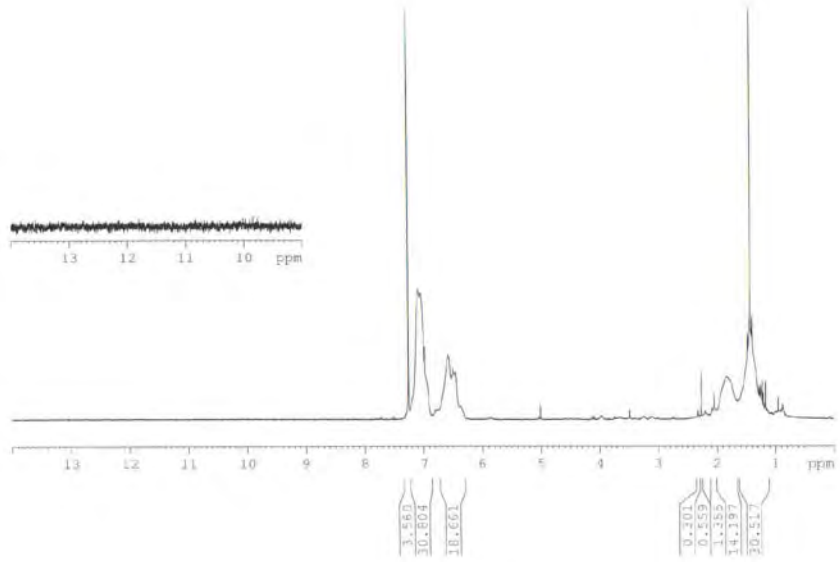

Figure 31: ^{1}H NMR spectrum of M-PS-2 after wash with TFA (400 mHz, $CDCl_3$). Note the absence of peaks at 13.1, 11.9 and 10.2 ppm corresponding to hydrogens of the ureidopyrimidinone groups.

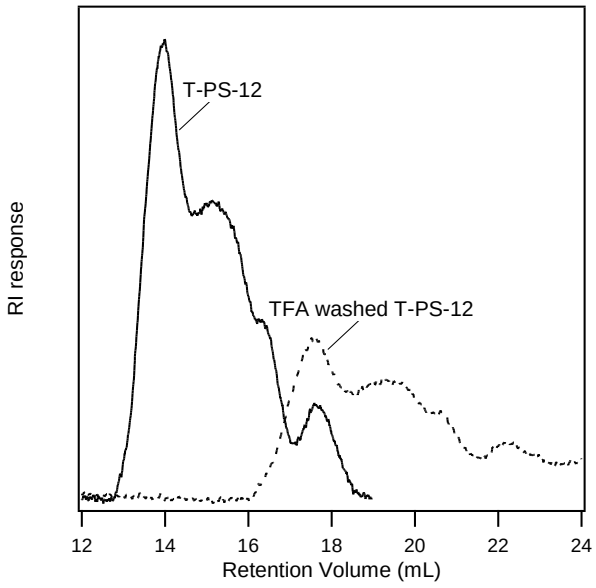

Figure 32: GPC chromatograms of T-PS-12 before and after TFA wash. Mobile phase was THF; column temperature 30 °C.

4.2 Differential Scanning Calorimetry

Differential Scanning Calorimetry measures thermal transitions such as melting and the glass transition. The incorporation of associating groups can affect the thermal transitions of the parent polymer. For crystalline polymers, a decrease in the melting temperature is expected with the incorporation of UPy end-groups as they can interfere with the molecular ordering. Associating end-groups, especially those capable of aggregating into stacks as seen by GPC can increase the glass transition temperature. The glass transition temperature, T_g, of a given polymer is an important consideration in miscibility studies. As a polymer is cooled below its T_g, it is frozen in a glassy state, locking in the phase structure that was present just above the highest T_g of the blend. Additionally, the glass transition temperature(s) of a blend system can be used as a measure of the miscibility of a blend (Section 6.1.3), but a knowledge of the T_gs of the individual components is needed first.

4.2.1 Instrumentation

Differential Scanning Calorimetry data was collected on a Perkin Elmer DSC 7 with Perkin Elmer Pyris Thermal Analysis Software, v. 6.0.0.0033. Heating/cooling rates were 20 °C/min. All thermograms shown are for the second heating.

4.2.2 Melting temperature

The DSC thermograms collected for a hydroxyl-terminated PEO before and after UPy-functionalization are shown in Figure 33. The incorporation of UPy end-groups onto PEO lowers melting temperature by 15 °C. This change in melting temperature is likely due to a disruption in the ordering of crystals of PEO by the associating ureidopyrimidinone end-groups. A depression in melting point upon UPy functionalization was also reported by van Beek[56] who investigated UPy functionalized polycaprolactones, poly(valerolactone)s and functionalized copolymers of the two. The melting points of the functionalized polymers were reduced relative to the hydroxyl-functionalized precursors.

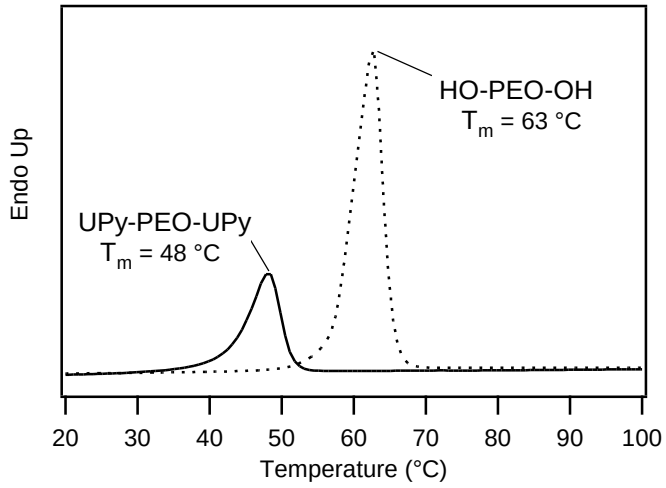

Figure 33: DSC Second heating thermograms of hydroxyl-terminated PEO and UPy-terminated PEO.

4.2.3 Glass transition temperature

The glass transition temperature, T_g, of a given polymer is an important consideration in miscibility studies. As a polymer is cooled below its T_g, it is frozen in a glassy state, locking in the phase structure that was present just above the highest T_g of the blend. Additionally, the glass transition temperature(s) of a blend system can be used as a measure of the miscibility of a blend (Section 6.1.3), but a knowledge of the T_gs of the individual components is needed first.

Differential Scanning Calorimetry was used to investigate the glass transition temperature of both UPy-functionalized polymers and polymer standards of comparable molecular weight. As shown in Figure 34 and 35 below, the attachment of UPy-end groups raises the glass transition temperature of the polymer. This is in agreement with results published in the literature. Hydrogen bonding,[94] and the incorporation of UPy groups[11, 95, 96] have both been reported to significantly raise polymer T_g.

The incorporation of UPy groups onto a single end of PMMA chains resulted in a 10 °C increase in glass transition temperature (Figure 34). DSC thermograms for several polystyrene samples are shown in (Figure 35). A larger increase in T_g was observed for M-PS-2. The magnitude of the change in T_g appears to be dependent on the mass fraction of end-group as T-PS-5 (which contains the same mass fraction of UPy end-groups) had a T_g nearly identical to M-PS-2, despite its increased molecular weight. A sample of monofunctional UPy-terminated polystyrene (M-PS-2) was washed with TFA (as described in section 4.2) to remove the associating UPy end-

groups. The DSC thermogram for this TFA washed sample is also shown in Figure 35. Removal of the UPy end-groups results in the decrease of the glass transition temperature to near the T_g measured for the 2.5 kDa standard sample. The association/stacking of UPy end-groups and/or the urethane linkages is likely decreasing the molecular mobility of the functionalized polymers resulting in the increased T_g.

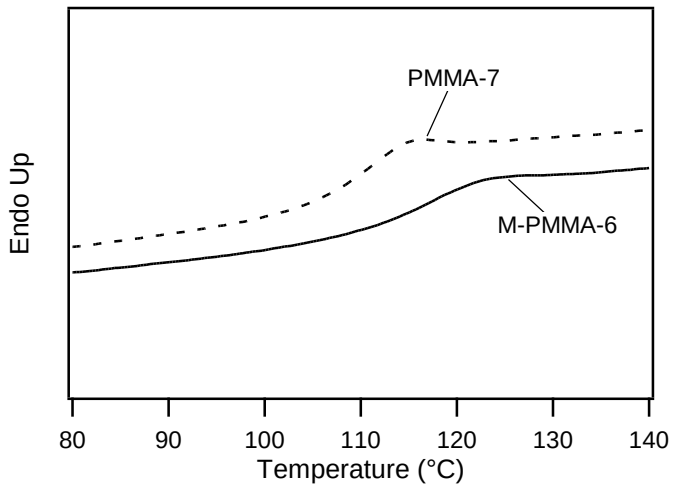

Figure 34: DSC thermograms of the second heating of PMMA-7 standard (dashed line) and M-PMMA-6 sample (solid line)**.**

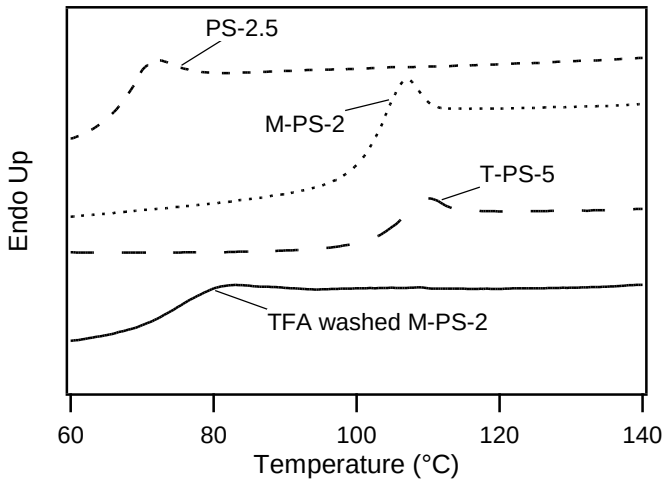

Figure 35: Second heating DSC thermograms of PS-2.5 standard (T_g = 69 °C), M-PS-2 (T_g = 104 °C), T-PS-5 (T_g = 107 °C) and TFA washed M-PS-2 (T_g = 75°C).

4.3 Conclusions

Gel Permeation Chromatography and Differential Scanning Calorimetry were used to characterize synthesized UPy-functionalized polymers. GPC chromatograms of telechelic materials showed significantly higher molecular weight than their monofunctional precursors, indicating successful coupling. In addition, low molecular weight telechelic samples showed multiple peaks corresponding to higher than expected molecular weights indicating possible aggregation of the polymer chains. This observed aggregation was attributed to association of UPy end-groups or the formation of end-group stacks via the urethane linkages. Experiments using a “chain stopper” to interfere with the formation of long chains of associated telechelic polymers only slightly changed the population distribution of aggregates, indicating that solution aggregates have a high stability.

Further GPC experiments were carried out in which the UPy end-groups were chemically cleaved from the polymer back bone using trifluoroacetic acid. TFA washing of telechelic samples resulted in GPC chromatograms that did not contain short retention volume peaks corresponding to aggregated polymer. To the best of our knowledge, this is the first time the aggregation of UPy end-groups has been observed by GPC.

TFA washing of monofunctional samples did not change the resulting GPC chromatograms. Therefore, the single peaks observed for monofunctional samples correspond to unassociated unimers and not associated dimers. The difference in the strength of the UPy association for monofunctional and telechelic materials is unclear, but cannot be attributed to the mass fraction of the UPy end-groups alone.

DSC was used to investigate the effect of the incorporation of UPy end-groups on polymer thermal properties. The incorporation of self-complementary UPy groups onto the ends of traditional polymers resulted in a decrease in melting temperature relative to its PEO precursor. This depression of the melting point is likely due to the disruption of the ordering of the crystalline PEO. For UPy-functionalized samples of PS and PMMA an elevation in T_g was observed compared to the analogous unfunctionalized polymer standard. The magnitude of the increase appears to be dependent upon the fraction of the polymer occupied by the associating end-groups. A higher concentration of end-groups has a larger effect on the polymer T_g. When the UPy groups were cleaved from the polymer backbone, the T_g of the resulting polymer returned to a temperature near that for the parent polymer standard.

Chapter Five: Miscibility of Blends Containing UPy-functionalized Polymers

Limited published research exists that examines the miscibility of blends incorporating supramolecular polymers. With an increasing number of potential applications being developed that incorporate supramolecular polymers,[8-10, 54, 55, 63] a more thorough understanding of the association of these materials and their miscibility in blends is needed. While it is known that the incorporation of specific interactions is one route to the enhancement of polymer miscibility,[29, 97] the effect of multiple hydrogen bonding end-groups on polymer blend miscibility has not been well studied.

This chapter will begin with a discussion of the techniques used to characterize blend miscibility. Next, the preparation of blend samples will be discussed. Lastly, the experimental observations of the miscibility of each polymer blend studied will be discussed. The order the studied blends are presented in was chosen to provide insight into motivation of the subsequent experiments.

5.1 Characterization techniques

The techniques utilized in the characterization of the phase behavior of selected blends and association of end-groups include DSC, optical microscopy, and laser light scattering. Details of these experimental techniques will be discussed briefly prior to discussion of our experimental findings.

5.1.1 Laser light scattering

Laser light scattering (LLS) is often used in miscibility studies.[35, 71, 98, 99] The apparatus for LLS experiments is relatively simple, and the use of custom built set-ups is not uncommon. In a typical miscibility experiment, a laser is shone onto the sample (solution or melt state), and temperature is increased or decreased until phase separation occurs. As the blend components begin to separate, domains form that scatter incident light. The phase separation temperature can be determined by the onset of either the increase in the intensity of scattered light, or the decrease in the intensity of transmitted light. The investigations of cloud point temperatures were carried out using a custom built laser light scattering apparatus (Figure 36). Blend sample tubes were centered in an aluminum cylinder equipped with three heater cartridges. Temperature was controlled with a Digi-Sense 68900 temperature controller. The sample was illuminated with a 635nm He-Ne laser and the scattered intensity at 90° to the incident beam was monitored using a photodiode detector. LabView software was used to record the scattered intensity and sample temperature.

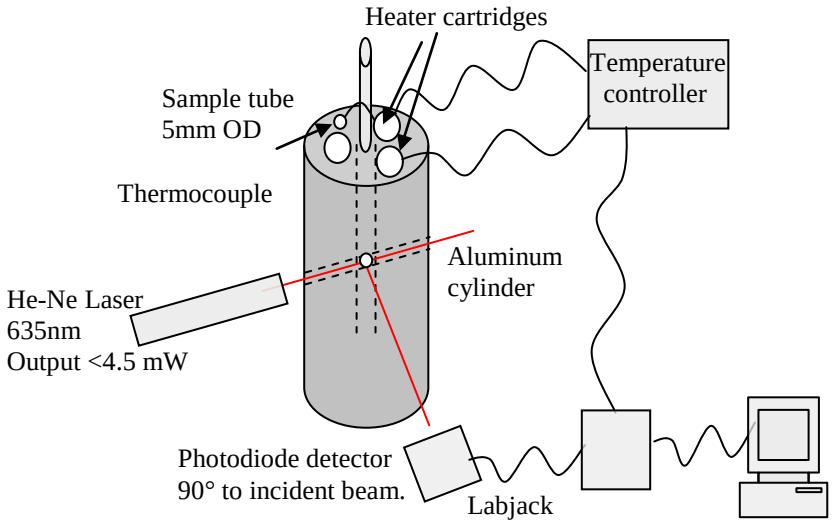

Figure 36: Illustration of 90 degree laser light scattering apparatus.

In a typical experiment for a UCST blend, the sample was slowly heated to a chosen temperature, soaked for 5-10 minutes, followed by slow cooling to room temperature. Temperature was cycled several times per experiment. The cloud point was determined as the temperature at which turbidity was observed upon cooling from the single phase region. An example of the data collected from laser light scattering is shown in Figure 37. Since the observed cloud point temperatures can be dependent upon heating/cooling rate, a rate of 0.1 °C/min was maintained near the transition temperature.

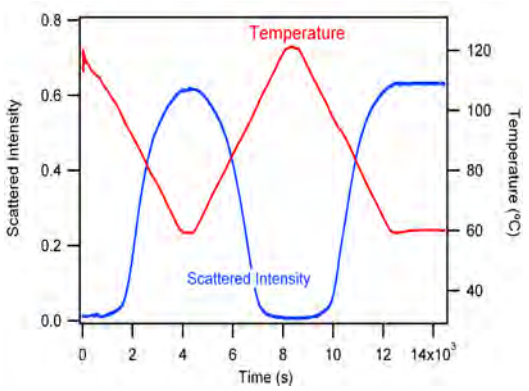

Figure 37: 90 degree LLS data for 50/50 PS/PB binary blend.

5.1.2 Optical microscopy

Hot–stage optical microscopy can be utilized in the study of blend miscibility. Under controlled heating/cooling, samples are observed for changes in turbidity. Upper critical solution temperatures are defined as the temperature at which the sample becomes clear on heating or the onset of turbidity upon cooling. If the blend to be studied contains a component that crystallizes, like PEO, crossed-polarizers can be used to further enhance image contrast.

Both isothermal and temperature ramp experiments were performed on blend samples. All studies were carried out using a Leica DML optical microscope. Isothermal observations were carried out at room temperature after annealing at elevated temperatures (see Section 6.2.4). For temperature ramp experiments, the microscope was equipped with a hot stage, the temperature of which was controlled using a Digi-Sense 68900 temperature controller. All digital images were acquired

using a Leica DFC 320 CCD camera. Sample heating/cooling rates were 2 °C/min unless otherwise stated.

5.1.3 Differential Scanning Calorimetry

Differential scanning calorimetry (DSC) is frequently used in the evaluation of the miscibility of blends.[100-102] The presence of a single glass transition temperature T_g, intermediate to the T_gs of pure components is regarded as an indication of blend miscibility. The appearance of separate, composition dependent T_gs is an indication of the presence of 2 phases of differing composition. Several well known equations which can be applied to the measured T_gs to determine the composition of the phases are shown below:

Gordon-Taylor equation:

$$T_g = \frac{w_1 T_{g1} + k w_2 T_{g2}}{w_1 + k w_2} \qquad k = \frac{\alpha_{1l} - \alpha_{1gl}}{\alpha_{2l} - \alpha_{2gl}} \qquad [5]$$

Fox equation

$$\frac{1}{T_{gm}} = \frac{w_1}{T_{g1}} + \frac{w_2}{T_{g2}} \qquad [6]$$

where w_i, T_{gi} are the weight fraction and glass transition temperature of component i, respectively. T_{gm} is the glass transition temperature of the blend. The parameter k, defined as the difference between the thermal expansion coefficient in the liquid and glassy states, is taken to be adjustable and an indication of intermolecular interaction strength.[103, 104] Behavior predicted by the Fox equation is usually expected for single

phase blends with little or no interaction between components. The Gordon-Taylor model has an adjustable parameter, *k*, which is related to the intensity of the interaction between blend components.

5.2 Blend characterization

5.2.1 Blend preparation techniques

Several approaches were used to prepare blend samples for miscibility studies. For hot stage optical microscopy, blends samples were cast onto 1" square glass slides. Cast films were dried in a vacuum oven for at least 12 hours. Drying temperatures ranged from 40 – 80 °C and were dependent upon the solvent used. Samples used for room temperature observations were prepared in a similar manner but employed standard 3" glass microscope slides and were annealed at temperatures above the T_gs of the individual components for two hours, followed by slow cooling (~1 °C/min) to room temperature prior to examination.

For laser light scattering, solution samples were prepared directly in the sample tube. Blend components were weighed as they were added to the sample tube. A small stir bar was added and the sample tube was heated, with stirring, to mix the sample. Sample tubes were sealed under vacuum prior to light scattering experiments. Binary melt state samples were prepared by first casting from solvent at room temperature and then placing the resulting film into the sample tube.

5.2.2 PS/PB system

As discussed previously in Section 2.2, the polystyrene/polybutadiene blend was chosen for study based on large interest from the rubber industry. Blends of these polymers are often chosen to utilize their phase separation into a multiphase morphology. The incorporation of associating end-groups, may afford greater control over the phase structures achievable in these blends. A thorough understanding of the miscibility of the functionalized polymers is therefore necessary.

Melt studies– Binary blends

Laser light scattering and optical microscopy were used to study the phase behavior of polybutadiene/polystyrene standard blends and telechelic UPy-functionalized polybutadiene (2.8 kDa)/polystyrene standard (2.5 kDa) blends. The cloud point data obtained by laser light scattering is shown in Figure 38. Cloud point temperatures were obtained across the entire composition range for the unfunctionalized parent blend. However, due to the limited thermal stability of polybutadiene, achieving well mixed blend samples containing telechelic UPy-PB-UPy without causing decomposition of the polybutadiene was difficult. Incorporation of UPy end-groups onto PB resulted in decreased miscibility with PS when compared with the unfunctionalized parent blend. The vast majority of functionalized blends studied decomposed prior to forming a single mixed phase. In fact, phase mixing was only observed with a 1/99 UPy-PB-UPy/PS blend which cleared at 65 °C. The equivalent unfunctionalized PB/PS blend cleared at 55 °C upon heating, but did not

phase separate upon cooling to room temperature, indicating that the sample is miscible at room temperature, but was not at equilibrium conditions prior to heat treatment.

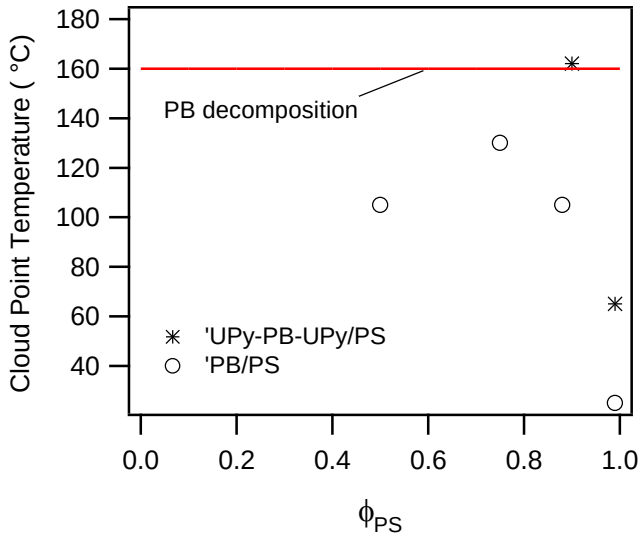

Figure 38: Cloud point temperatures for PS/PB binary blends. Point appearing above PB decomposition line indicates sample decomposed before mixing.

The difficulties in obtaining a phase mixed sample in the UPy-PB-UPy/PS system led to the investigation of the miscibility of UPy-PB-UPy with the unfunctionalized PB standard. A 1/99 UPy-PB-UPy/PB blend did not form a homogeneous single phase prior to decomposition at 160 °C.

Solution studies – Ternary blends with toluene

Given the difficulty in obtaining functionalized blends with phase transitions at experimentally accessible temperatures (and before decomposition), ternary solutions with a solvent were investigated. Laser light scattering was used to study the phase behavior of blends of UPy-functionalized polystyrene with a polybutadiene standard (2,800 g/mol) in toluene. Toluene was chosen for its relatively low volatility and ability to solubilize both blend components. Blend samples were prepared directly in the sample tube and the tube was sealed under vacuum prior to heating. Table 6 shows the measured cloud point temperatures for blends of polystyrenes with varying UPy-functionalization with the PB standard. The greatest decrease in miscibility relative to the parent blend was observed when the UPy-functionalized polystyrene was telechelic. The PS standard used in these studies was a higher molecular weight (12,400 g/mol) than that used in the melt studies. This increased molecular weight was chosen to enable a more direct comparison of parent blend behavior to the behavior of the analogous blend with monofunctional UPy-PS. Assuming the formation of dimers, the molecular weight of the PS components of the blends should be equivalent. As shown in Figure 39, the behavior of blends with UPy-PS-Br (6 kDa) is very similar to blend with 12 kDa PS standard. In fact, for monofunctional UPy-polymers, it was expected that the miscibility should be comparable to the miscibility for the parent polymer of twice the molecular weight (corresponding to the formation of dimers by the functionalized polymer). Examination of Figure 39 shows the transition is broader for the blend with the UPy-

PS than for the PS/PB standard blend. Also of interest, the minimum scattered intensity (clear, phase mixed sample) appears to be increased in the presence of UPy groups. Previously reported stacking of UPy groups may explain this observation.[21]

Table 6: Summary of LLS data for ternary blends of various PSs with PB standard (2,800 g/mol) in toluene.

Polystyrene component			
Type	M_n (g/mol)	PS/PB/toluene	Cloud Point Temperature (°C)
PS-12	12,400	37/3/60	35
M-PS-6	6,000	37/3/60	38
T-PS-12	12,000[a]	37/3/60	> 140
T-PS-12	12,000[a]	34/6/60	> 140
M-PS-6	6,000	28/12/60	55

a) GPC chromatogram for this showed multiple peaks determined to be due to aggregation of the end groups. M_n listed is M_n of unassociated polymer.

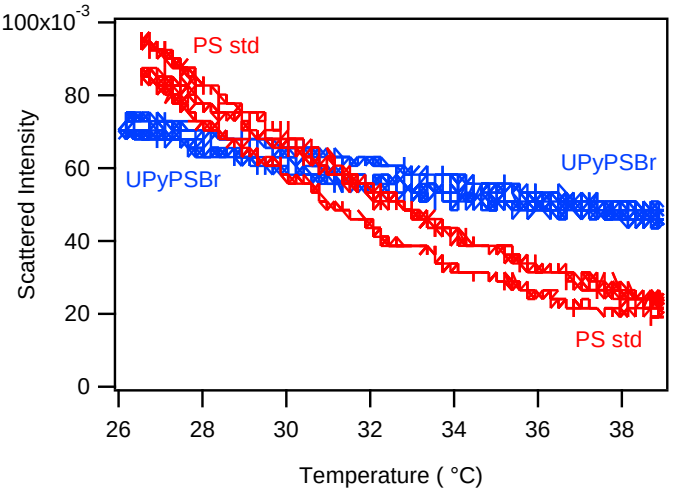

Figure 39: Light scattering data for ternary blends of 54/6/60 PS/PB/toluene and 54/6/60 M-PS-6/PB/toluene.

5.2.3. PS/PDMS system

The poor mechanical properties of PDMS often necessitate the incorporation of glassy fillers (such as PS) as reinforcing materials. Commercialization of a PS/PDMS blend has not yet been achieved. The incorporation of associating end-groups may enhance the miscibility of this polymer pair, making it commercially viable.

Binary blends of polystyrene with poly(dimethylsiloxane) were characterized using laser light scattering. For this system, blends containing two supramolecular polymers bearing the same self-complementary UPy end-groups were compared with blends of the unfunctionalized parent polymers. Blends were prepared of 8% telechelic UPy-functionalized PDMS (2,300 g/mol) and 92% telechelic UPy-functionalized PS (3,600 g/mol). Samples for LLS were prepared by casting from chloroform solutions (5% solids). Films were cast into Bytac boats and dried overnight in a 50 °C vacuum oven. Resulting films were broken up and placed into light scattering sample tubes. The incorporation of UPy end-groups onto both polymers resulted in decreased miscibility compared with unfunctionalized parent blend. A 10/90 PDMS/PS unfunctionalized standard blend was observed to form a homogeneous single phase at 90 °C; while the analogous UPy-PDMS-UPy/UPy-PS-UPy blend showed a clearing temperature greater than 160 °C. For UCST systems, the samples at the extremes of the composition range have the lowest clearing temperatures. Given this fact, and that above 160 °C, degradation begins to interfere

with the formation of a miscible blend; the remaining blend compositions were not individually studied. It was concluded that telechelic functionalization of both polymers of the blend results in a decrease in miscibility for this polymer pair.

5.2.4. PS/PMMA system

Blends of PS with PMMA have been widely characterized previously, allowing for the calculation of predicted phase diagrams for blends of PS and PMMA standards. For this blend system, several different functionalized blends were explored: mono-functional PS with PB standard, PS standard with mono-functional PB, blends where both polymers are mono-functionalized and blends where both polymers are telechelic.

Given the numerous samples to be discussed for this blend system, abbreviated sample names were chosen to provide the following information: architecture ("M" for mono-functional or "T" for telechelic), backbone type (ex., "PS" or "PMMA"), and molecular weight (in kDa).

Melt studies– Binary blends

Films of blended samples were prepared by dissolving polymers into dichloromethane and casting onto glass microscope slides. The average film thickness was measured to be about 30 μm. Cast blends were allowed to dry, and the resulting films were vacuum-annealed (150 °C) for two hours to completely remove

the solvent and overcome phase separation that may be due to solvent evaporation. The annealing temperature was chosen to be above the glass transition temperature of both blend components. Samples were then slow-cooled (~1°C /min) to room temperature and were inspected using optical microscopy. Since room temperature is well below the glass transition temperature (T_g) of both components, this method indicates the phase state at a temperature immediately above the highest T_g of the blend's components.

PS/M-PMMA blends

This section will present results for blends of "parent" polystyrene standards of varying molecular weight with a monofunctionalized PMMA sample (M-PMMA-6). The characteristics of monodisperse standards used in are shown in Table 7.

Figure 40 displays typical microscope images for two cast PS/M-PMMA blends. A clear distinction between phase-mixed and phase-separated states was apparent for all blends studied. The length scale of phase separation was about 15 μm, and phase-separated blends generally appeared darker because more light was scattered by the presence of interfaces. Interestingly, phase-separated films were often more brittle than homogeneous films, and cracks were frequently observed. This may be due to the presence of interfaces between the phase-separated domains, along which crack propagation can more easily occur.

Table 7: Polymer standards used in PS/PMMA blend studies.

Polymer	M_n (g/mol)	PDI
PS-2	2,400	1.01
PS-4	4,100	1.02
PS-10	10,000	1.03
PS-12	12,500	1.06
PMMA-7	6,700	1.04
PMMA-22	22,200	1.26

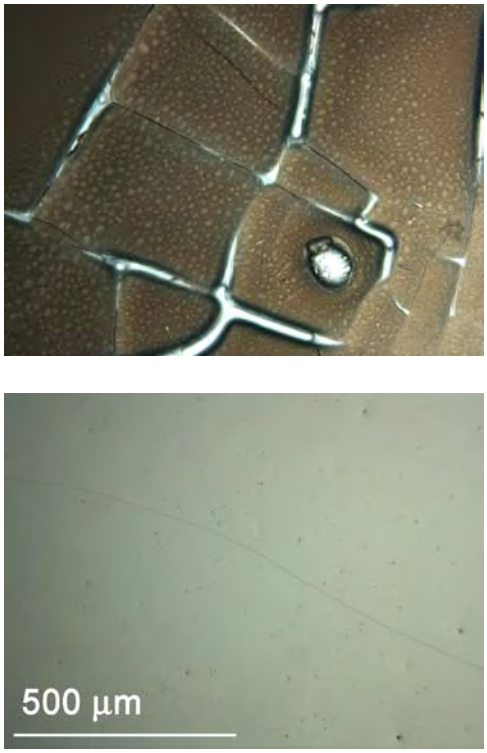

Figure 40: Microscope images of cast blend films of 50/50 PS-4/M-PMMA-6 (top) and 50/50 PS-2/M-PMMA-6 (bottom) showing examples of demixed and mixed states, respectively. The scale bar is the same for both images.

To compare miscibility of end-functionalized polymers with their parent blends, the product of the Flory-Huggins interaction parameter χ and the average degree of polymerization N_{ave} was plotted against volume fraction, ϕ (*e.g.* Figure 41). Since blends often involved two polymers with different molecular weights, the average degree of polymerization, N_{ave}, was taken to be [105]

$$N_{ave} = \left(\frac{1}{\sqrt{N_A}} + \frac{1}{\sqrt{N_B}} \right)^{-2} . \qquad [3]$$

The occurrence of the critical point at $\chi N_{ave} = 0.5$ is a consequence of using Equation 3 to define the degree of polymerization. Below the critical point the parent blends should exhibit complete miscibility. Values of χ for parent PS/PMMA blends were calculated from the literature[82] according to $0.028 \pm 3.9/T$ using a temperature of 100 °C which is close to the T_g of both components. This empirical model of χ was also used when plotting observed miscibility for functionalized polymers. Clearly, this is an approximation since the end-groups occupy a fraction of the backbone and therefore will alter χ. Nevertheless the approach enables blends containing UPy end-groups to be directly compared to their parent blends.

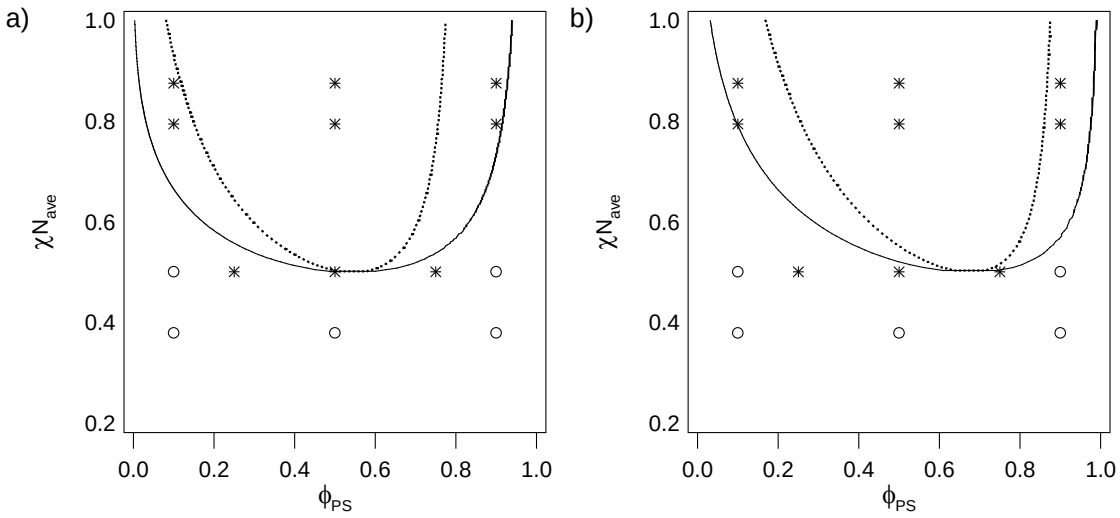

Figure 41: Room temperature observations of miscibility of unfunctionalized polystyrenes of varying molecular weight with M-PMMA-6. Open symbols indicate phase-mixed observations. Dashed and solid lines are spinodal and binodal predictions for blends containing a) 6.3 kDa PMMA and b) 12.6 kDa PMMA.

Figure 41 is a summary of room-temperature observations and compares the phase behavior of PS/M-PMMA blends to the predicted miscibility of unfunctionalized parent PS/PMMA blends. This figure displays the observed miscibility of fourteen different blends of PS/M-PMMA-6 following casting, cooling, and annealing. The four different vertical positions correspond to blends prepared using different PS standards (PS-2, PS-4, PS-10, and PS-12). M-PMMA-6 forms homogeneous blends at all compositions when processed with the lowest molecular weight polystyrene. Figure 41a shows the binodal (solid line) and spinodal (dotted line) stability limits of parent blends containing PS and 6.3 kDa PMMA (the same molecular weight at M-PMMA-6). The spinodal line was calculated using the Flory-Huggins equation of state model and the stability criterion $\partial^2 \Delta G_m / \partial \phi^2 = 0$ where

ΔG_m is change in free energy upon mixing. The binodal line, which indicates the location of the metastable region of the phase diagram, was determined by finding the points of double tangency on a plot of ΔG_m vs ϕ.

The functionalized blends show demixing beneath the parent blend's stability curve, *i.e.* in the predicted single-phase region, indicating a decrease in PS/PMMA blend miscibility. This observation is qualitatively consistent with the prediction that end-group interactions can stabilize two-phase regions.[58] However, it is not clear whether this effect is due to solely to end-to-end association. Demixing may also be promoted because of enthalpic differences—the interaction parameter between PS and M-PMMA-6 may exceed that between PS and PMMA.

To determine if the observed decrease in miscibility is due to the increased molecular weight upon formation of dimers of M-PMMA-6, experimental data was compared with predictions for blends of PS and 12.6 K PMMA—the same molecular weight as dimers of associated M-PMMA-6. Figure 41b shows the binodal solid line) and spinodal (dotted line) stability limits of parent blends containing this higher molar mass PMMA. Again, the functionalized blends show demixing within the predicted single-phase region. Therefore, the observed decreased miscibility cannot be attributed to increase in molecular weight alone (upon association to form dimers). The stabilization of the two-phase region of the phase diagram is likely due to a combination of end-to-end association, the formation of stacks by hydrogen bonding of the adjacent urethane linkages, and enthalpic differences between UPy end-groups and homopolymers.

While optical microscopy offers easy sample preparation and small sample sizes, it can be limited by the size of the phase-separated domains. In samples where phase separation has occurred, but domain sizes are too small to be imaged using optical microscopy, samples may appear to form a single, mixed, phase when they are in fact phase-separated. In light of this concern, DSC experiments were used to selectively corroborate optical microscopy results. DSC data were collected for blends of PS-4 with M-PMMA-6 as well as for the pure materials. Results are shown in Figure 42. In good agreement with optical microscopy data in Figure 41, single T_gs were observed for the 90/10 and 10/90 blends and two separate T_gs for the 49/51 blend.

Neither the Gordon-Taylor [4] nor Fox [5] equations for the T_g of blends (section 6.1.3) agrees with the T_gs of the blend samples shown in Figure 42. For the phase mixed samples (90% PS-2.5 and 10% PS-2.5), the Fox equation predicts T_gs of 72 °C and 109 °C, respectively. The measured T_gs are 89 °C and 122 °C. The Fox equation is not typically applied to blend systems with specific interactions. The Gordon-Taylor equation has an adjustable parameter, *k*, which is supposedly indicative of the interactions between blend components. When the Gordon-Taylor equation is applied to the 90% PS-2.5 and 10% PS-2.5 blends, very different values are obtained for the parameter *k* (6.4 and -1.1 respectively). The value of k is not reported to be composition dependent and should be constant for a given blend pair.

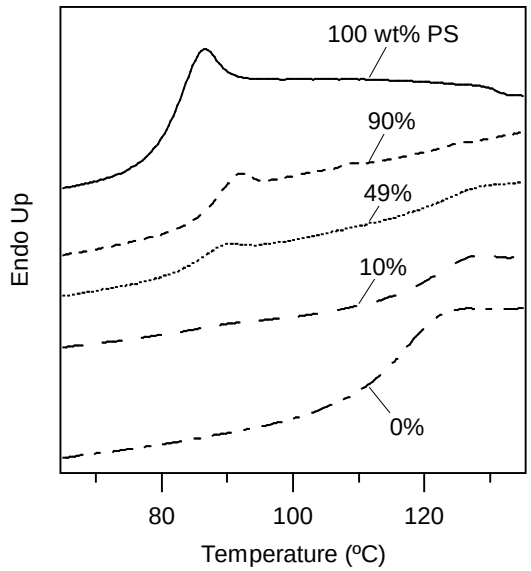

Figure 42: DSC second heating thermograms for PS-4, M-PMMA-6, and their blends.

M-PS/PMMA blends

Ten blends were also prepared in which mono-functional polystyrene (M-PS-2) was mixed with various PMMA standards. Optical microscopy results are shown in Figure 43. The two different vertical positions correspond to blends prepared using PMMA-7, and PMMA-22. Figure 43a shows the binodal (solid line) and spinodal (dotted line) stability limits of parent blends containing PMMA and 2.4 kDa PS (the same molecular weight as M-PS-2). Figure 43b shows the binodal (solid line) and spinodal (dotted line) stability limits of parent blends containing PMMA and 4.8 kDa PS (the same molecular weight as dimers of associated M-PS-2). As described in the discussion of Figure 41, these lines were calculated using the Flory-Huggins equation of state model and the stability criterion. M-PS-2 formed homogeneous blends at all

compositions except the 50/50 blends when processed with either weight poly(methyl methacrylate) standard. As seen for the PS/M-PMMA blends, the experimental miscibility differs from the predictions for the parent blend. Experimental observations of miscibility differ significantly from predictions based on unimers of M-PS-2 (Figure 43a) as well as predictions based on dimers of M-PS-2 (Figure 43b). Slightly better agreement with predictions is observed when molecular weight of dimers is considered.

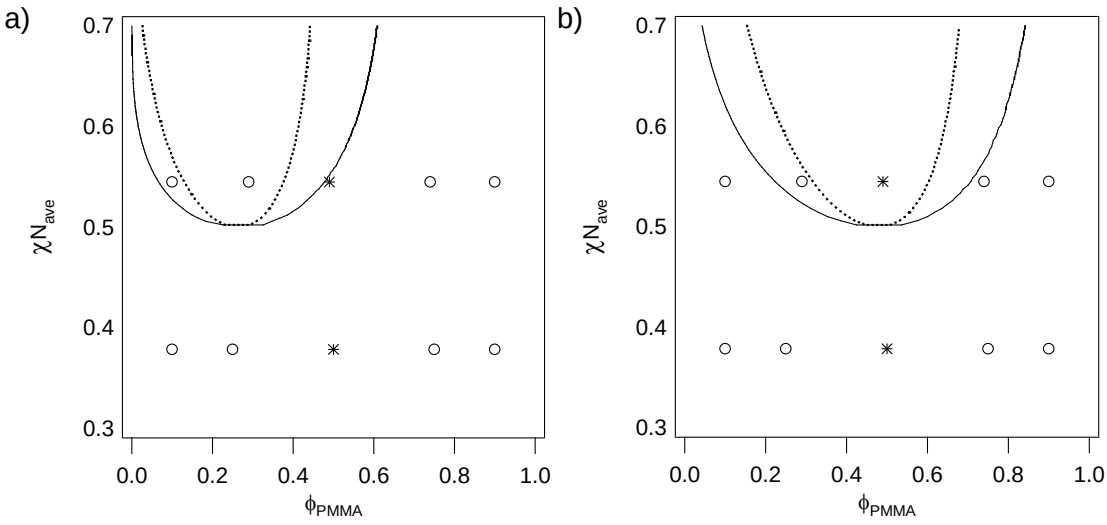

Figure 43: Room temperature observations of miscibility of PMMA-7 and PMMA-27 with M-PS-2. Open symbols indicate phase-mixed observations. Dashed and solid lines are spinodal and binodal predictions for blends containing a) 2.4 kDa PS and b) 4.8 kDa PS.

M-PS/M-PMMA blends

The miscibility of blends in which both components were mono-functional was also investigated. Optical microscopy results are shown in Figure 44 which again shows predicted binodal (solid line) and spinodal (dotted line) stability limits of parent blends containing PS and 13 kDa PMMA.(the same molecular weight as M-PMMA-13). As in above figures, the prediction was calculated using the Flory-Huggins equation of state model and the stability criterion. As indicated by the observation of phase separation within the predicted single phase region, there is a reduction in miscibility observed for these blends even though inter-association, as well as self-association, by hydrogen bonding is possible. Additionally, experimental observations display asymmetry in the phase diagram that is consistent with the predictions.[58]

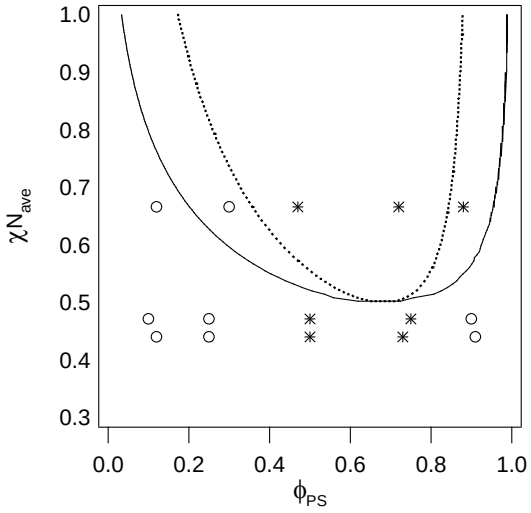

Figure 44: Room temperature observations of miscibility of M-PSs with M-PMMAs of varying molecular weights. Open symbols indicate phase-mixed observations. Dashed and solid lines are spinodal and binodal predictions for blends of PS with 13 kDa PMMA.

T-PS/T-PMMA blends

Telechelic materials prepared by ATRC were also used in PS/PMMA blend studies. All blends containing telechelic materials were immiscible. For example, blends of T-PS-9 with T-PMMA-13 were immiscible across the entire composition range. We attribute this either to end-to-end association of telechelic polymers to form longer chains or to the stacking of UPy end-groups.[48] Considering our GPC observations discussed in the Chapter 4, low molar mass telechelic polymers are more prone to forming aggregates, even in solution. These aggregates are remarkably stable and are able to pass through elevated-temperature (60 °C) chromatography columns. Given this observation of aggregates in solution, aggregates are likely present at the time of casting, which would kinetically hinder the formation of a single mixed phase upon annealing. Nevertheless, end-to-end association or stacking of end-groups should result in blend components with greater effective molecular weights, partly explaining the observed decrease in miscibility.

5.3 Conclusions

Several techniques were employed to investigate the miscibility of blends incorporating UPy end-functionalized polymers. The miscibility of the functionalized blends was then compared the miscibility of analogous traditional polymer-polymer blends. Blends studied included PS/PB, PS/PDMS and PS/PMMA. The cloud point temperatures of PS/PB and PS/PDMS blends were investigated using a custom built

laser light scattering apparatus. In both cases, functionalization of either (or both) components of the blend decreased the miscibility relative to the parent blend.

Blends of PS/PMMA, studied by optical microscopy and DSC, also showed a decrease in miscibility as a result of UPy functionalization. In fact, blends containing one monofunctional component showed decreased miscibility even when compared with predictions for parent polymers of twice their molecular weight (corresponding to the formation of dimers). Therefore, the observed decrease in miscibility cannot be solely attributed to the increased molecular weight from end-group association.

Feldman *et al*. previously reported miscibility of low T_g, (meth)acrylic polymers containing mono-functional UPy and 2,7-diamido-1,8-naphthyridine (Napy) end-groups.[52] Their study showed that the phase behavior is largely influenced by end-group specificity. Blends with each component containing a self-complementary UPy end-group showed slight compatibilization, whereas blends containing UPy – Napy (hetero-complementary) groups lead to significant retardation of phase separation. For the PS/PMMA system, two high T_g polymers were considered containing self-complementary UPy end-groups. The observed miscibility is indicative of the phase-state near the highest T_g — typically ~ 100 °C. However, the equilibrium degree of association near 100 °C may be significantly lower than that occurring near room temperature, and this may limit the ability of hydrogen-bonding end-groups to compatibilize the blend. Furthermore, kinetic issues may be important. On the one hand, around 100 °C, UPy-groups have much higher dissociation rates than at room temperature, and this should promote more rapid equilibration of phase-

state. On the other hand, unlike the Feldman study, the self-complementary end-groups are connected to the polymer backbone using urethane linkages that, in addition to end-to-end association, are capable of intermolecular stacking.[48] The present study highlights that decreased miscibility is not due to end-to-end association alone. Enthalpic differences between end-groups and backbones as well as end-group aggregation may play equally important roles.

Chapter Six: Suggested Future Research

Based on our experimental findings, three main areas of future research are recommended. Further investigation of the effect of the urethane linkage adjacent to the UPy end-group, investigation of the effect of hetero-complementary associations on blend miscibility and investigation of UPy functionalized blends with component Tgs at or below room temperature are all recommended. In this section, each of these research recommendations will be discussed individually although there is overlap between the topics of suggested research.

6.1 Investigation of the effect of urethane adjacent to UPy end-group

Our data indicate that functionalization with self-complementary hydrogen bonding end-groups incorporating a urethane linkage, onto one or both polymers of a blend will decrease the miscibility of the blend compared to the parent polymer blend. In the current work it is not determined if the decreased miscibility observed is due to the association of UPy end-groups, the stacking of end–groups through urethane linkages, or a combination of the two effects. Future work should include the study of blends containing UPy end-groups *without* the additional urethane linkage present. Specifically, analogous blends of the same UPy-functionalized polymers with and without the additional urethane linkage should be prepared. A direct comparison of blends which differ only in the presence of the urethane linkages would allow clarification of the impact of self-associating end-groups on the miscibility of traditional polymer-polymer blends.

In order to prepare UPy-functionalized polymers without the urethane linkage, the imidazole chemistry discussed in Section 3.2 would need to be utilized. Using the UPy-imidazole, a new functionalized ATRP initiator could be synthesized from 2-aminoethyl-2-bromoisobutyrate initiator (Figure 45). The synthesis of the amino terminated precursor has been previously reported in the literature.[106] UPy-functionalized polystyrenes prepared by this method should be blended with polymer standards to repeat previously studied blend systems. This would allow a direct comparison of the impact of the UPy group with and without the urethane linkage present. Additionally, the GPC experiments detailed in Chapter 4 should be repeated with the urethane-free PS samples to determine the origin of the aggregation observed in several samples in this work. If aggregation is still observed, then it can be attributed to the association of telechelic samples into longer chains, as opposed to the formation of stacks in the presence of the urethane linkage.

Figure 45: Synthesis of urethane-free UPy-bromoisobutyrate ATRP initiator.

6.2 Blends containing hetero-complementary associating end-groups

Experiments should be carried out that study blends containing hetero-complementary hydrogen bonding end-groups such as the UPy-Napy system (Figure 46) discussed earlier. The Napy functionality has been shown to disrupt self-associated UPy dimers in favor of cross association.[65] The only published studies dealing with the miscibility of systems incorporating UPy-Napy associations considers only *monofunctional* samples.[52] As reported from initial studies by Feldman[52] et al, the introduction of these UPy and Napy groups onto a single end of a polymer chain, greatly suppresses phase separation. The study of *telechelic* materials containing these end groups would be the first of its kind and could show even greater compatibilization of unlike polymers as well as the generation of interesting and unique microstructures resulting from microphase segregation into phase separated domains.

Figure 46: UPy-Napy hetero-complementary association through hydrogen bonding (dashed lines).

Given the demonstrated enhancement of miscibility with this hetero-complementary pair, it would also be interesting to functionalize both components of a blend known to be immiscible to determine if it is possible to compel miscibility in an immiscible system with hydrogen bonding end-groups.

6.3 Investigation of functionalized blends comprised of low T_g polymers

One of the difficulties in the current research arises from the choice of polystyrene for our polymer blends. Polystyrene was chosen based on the ability to prepare functionalized polymers by ATRP/ATRC. However, polystyrene has a T_g well above room temperature at 100 °C. Studying blends with T_gs well above room temperature can hinder the ability to observe changes in phase behavior. In the interest of being able to observe the onset of clearing/turbidity of studied blends, the selection of a blend of low T_g polymers is recommended. Ideally, the components of the selected polymer blend would have low T_gs and be able to be prepared using the ATRP/ATRC techniques developed in this work. One possible blend system for further study is poly(n-butyl acrylate)/poly(methyl acrylate). Both materials posses low T_gs and can be synthesized by ATRP/ATRC. Because ATRP/ATRC can be used to synthesize both of the blend components, this blend facilitates the investigation of miscibility of polymers with self-associating hydrogen bonding end-groups with and without the urethane linkage present to assess the impact of the formation of lateral stacks on blend miscibility.

Table 8: Suggested PnBA/PMA blends for future miscibility studies.

End-group on PnBA	End-group on PMA	Motivation
UPy with urethane linkage	UPy with urethane linkage	Low Tgs should allow for observation of clearing
UPy without urethane	UPy without urethane	For direct comparison with UPy *with* urethane linkage
UPy	Napy	Investigation of effect of hetero-complementary associations

Chapter Seven: Conclusions

UPy-functionalized monofunctional and telechelic polymers were successfully prepared for use in polymer blend studies. Several different synthetic routes were utilized in the preparation of UPy-polymers. The most versatile and successful approach was the use of ATRP/ATRC. A ureidopyrimidinone functionalized ATRP initiator was prepared for use in ATRP reactions. ATRP carried out using this functionalized initiator guaranteed that each polymer chain grown would bear the UPy functionality at one chain end. These monofunctional polymers were then coupled by ATRC to form telechelic UPy-functionalized samples. Molecular weight control was achieved by varying the ratios of reactants and by changing the reaction time.

The presence of the UPy end-groups was shown to affect the physical properties of the parent polymers. Several parent polymers that were liquids prior to functionalization increased in viscosity to become viscous liquids or waxy solids upon UPy functionalization. The thermal properties of UPy-functionalized polymers were also investigated. Functionalization of poly(ethylene glycol) with UPy end-groups lowered the melting point of the PEG by 15 °C. Additionally, several PS samples (monofunctional and telechelic) showed an increased T_g upon incorporation of UPy end-groups. The magnitude of the T_g shift appears to be related to the fraction of the polymer occupied by the UPy end-groups, with M-PS-2 and T-PS-5 displaying the same T_g. Cleavage of the UPy groups from the polymer backbone resulted in the T_g returning to near the T_g of the unfunctionalized parent.

GPC data acquired for the functionalized polymers suggest the formation of aggregates/stacking for low molecular weight, telechelic polymers. While single peaks were observed for monofunctional samples, multiple low retention volume (high molecular weight) peaks were observed for two low molecular weight telechelic PS samples. These lower retention volume peaks appear to correspond to integer multiples of the expected unassociated polymer molecular weight. The addition of a short UPy-containing "chain stopper" to impede association only slightly changed the distribution of the GPC chromatogram, indicating that the aggregates are highly stable in solution. When the associating UPy end-groups were chemically cleaved from the ends of telechelic samples, no GPC peaks were observed that correspond to association/aggregation. To the best of our knowledge, this work is the first time that association/aggregation of UPy end-groups by GPC has been observed.

Motivated largely by the lack of published research addressing the impact of the incorporation of hydrogen bonding end-groups, one of our objectives in this work was to investigate the effect of the UPy end-groups on the miscibility of traditional polymer-polymer blends. The miscibility of blends containing UPy-functionalized polymers as well as the parent homopolymer standard blends were studied in solution and in the melt state. For blends containing one polymer that was monofunctional and one parent standard polymer, miscibility was generally decreased although phase-mixed samples were observed. The miscibility of these blends was decreased even when compared with polymer standards of molecular weights corresponding to dimers of the monofunctional polymer. Therefore, the decreased miscibility cannot be solely attributed to the increased molecular weight from association. Our polymers

contain a urethane linkage adjacent to the UPy end-groups. The presence of this urethane linkage has been reported by others to result in stacking of the end-groups into aggregates.[48] It is our conclusion that the decreased miscibility of our UPy-functionalized polymers likely stems from a combination of association, stacking and enthalpic differences between the UPy end-group and the polymer backbones.

When both blend components contained single UPy end-groups, miscibility was decreased despite the opportunity for cross-association between the blend components. In blends which contained one or both telechelic, UPy-functionalized polymer(s) immiscibility was observed across the entire composition range. Based on our blend studies, the incorporation of self-complementary ureidopyrimidinone end-groups decreases the melt miscibility of traditional polymer-polymer blends. Several other blend experiments were suggested to provide additional insight into the miscibility of end-associating polymers.

References

1. Lehn, J.-M. *Prog. Polym. Sci.* **2005,** 30, 814–831.

2. Brunsveld, L.; Folmer, B. J. B.; Meijer, E. W.; Sijbesma, R. P. *Chem. Rev.* **2001,** 101, (12), 4071–4097.

3. Blasini, D. R.; Flores-Torres, S.; Smilgies, D.-M.; Abruna, H. D. *Langmuir* **2006,** 22, (5), 2082–2089.

4. Bosman, A. W.; Brunsveld, L.; Folmer, B. J. B.; Sijbesma, R. P.; Meijer, E. W. *Macromol. Symp.* **2003,** 201, 143–154.

5. Fouquey, C.; Lehn, J.-M.; Levelut, A.-M. *Adv. Mater.* **1990,** 2, (5), 254–257.

6. Ciferri, A., *Supramolecular Polymers*. Marcel Dekker, Inc.: New York, 2000.

7. Rieth, S.; Baddeley, C.; Badjic, J. D. *Soft Matter* **2007,** 3, 137–154.

8. Cordier, P.; Tournilhac, F.; Soulie-Ziakovic, C.; Liebler, L. *Nature* **2008,** 451, 977–980.

9. Li, J.; Viveros, J. A.; Wrue, M. H.; Anthamatten, M. *Adv. Mater.* **2007,** 19, 2851–2855.

10. Kautz, H.; van Beek, D. J. M.; Sijbesma, R. P.; Meijer, E. W. *Macromol.* **2006,** 39, (13), 4265–4267.

11. Yamauchi, K.; Lizotte, J. R.; Hercules, D. M.; Vergne, M. J.; Long, T. E. *J. Am. Chem. Soc.* **2002,** 124, (29), 8599–8604.

12. Rieth, L. R.; Eaton, R. F.; Coates, G. W. *Angew. Chem. Int. Ed.* **2001,** 40, (11), 2153–2156.

13. Hirschberg, J. H. K. K.; Ramzi, A.; Sijbesma, R. P.; Meijer, E. W. *Macromol.* **2003,** 36, 1429.

14. Sherrington, D. C.; Taskinen, K. A. *Chem. Soc. Rev.* **2001,** 30, 83–93.

15. Farnik, D.; Kluger, C.; Kunz, M. J.; Machl, D.; Petraru, L.; Binder, W. H. *Macromol. Symp.* **2004,** 217, 247–266.

16. Hirschberg, J. H. K. K.; Beijer, F. H.; van Aert, H., A.; Magusin, P. C. M. M.; Sijbesma, R. P.; Meijer, E. W. *Macromol.* **1999,** 32, (8), 2696–2705.

17. Ligthart, G. B. W. L.; Ohkawa, H.; Sijbesma, R. P.; Meijer, E. W. *J. Am. Chem. Soc.* **2005,** 127, (3), 810–811.

18. Kuo, S.-W.; Chan, S.-C.; Chang, F.-C. *Macromol.* **2003,** 36, 6653–6661.

19. Jorgensen, W. L.; Pranata, J. *J. Am. Chem. Soc.* **1990,** 112, 2008–2010.

20. Pranata, J.; Wierschke, S. G.; Jorgensen, W. L. *J. Am. Chem. Soc.* **1991,** 113, 2810–2819.

21. Folmer, B. J. B.; Sijbesma, R. P.; Kooijman, H.; Spek, A. L.; Meijer, E. W. *J. Am. Chem. Soc.* **1999,** 121, (39), 9001–9007.

22. Sijbesma, R. P.; Beijer, F. H.; Folmer, B. J. B.; Hirschberg, J. H. K. K.; Lange, R. F. M.; Lowe, J. K. L.; Meijer, E. W. *Science* **1997,** 278, 1601–1604.

23. Beijer, F. H.; Sijbesma, R. P.; Kooijman, H.; Spek, A. L.; Meijer, E. W. *J. Am. Chem. Soc.* **1998,** 120, (27), 6761–6769.

24. Beijer, F. H.; Kooijman, H.; Spek, A. L.; Sijbesma, R. P.; Meijer, E. W. *Angew. Chem. Int. Ed.* **1998,** 37, 75–78.

25. Corbin, P. S.; Zimmerman, S. C. *J. Am. Chem. Soc.* **1998,** 120, 9710–9711.

26. Luning, U.; Kuhl, C. *Tetrahedron Lett.* **1998,** 39, 5735–5738.

27. Zeng, H.; Miller, R. S.; Flowers, R. A.; Gong, B. *J. Am. Chem. Soc.* **2000,** 122, (11), 2635–2644.

28. Yang, X.; Martinovic, S.; Smith, R. D.; Gong, B. *J. Am. Chem. Soc.* **2003,** 125, 9932–9933.

29. Olabisi, O.; Robeson, L. M.; Shaw, M., T, *Polymer-polymer miscibility*. Academic Press: New York, 1979.

30. Sperling, L. H., *Polymeric Multicomponent Materials: An Introduction*. John Wiley & Sons, Inc.: New York, 1997.

31. Lipatov, Y. S.; Nesterov, A. E., *Thermodynamics of Polymer Blends*. Technomic Publishing Company, Inc.: Lancaster, 1997; Vol. 1.

32. Flory, P. J., *Principles of Polymer Chemistry*. Cornell University Press: Ithaca, 1953.

33. He, Y.; Zhu, B.; Inoue, Y. *Prog. Polym. Sci.* **2004,** 29, 1021–1051.

34. Coleman, M. M.; Painter, P., C. *Prog. Polym. Sci.* **1995,** 20, 1–59.

35. Haraguchi, M.; Nakagawa, T.; Nose, T. *Polym.* **1995,** 36, (13), 2567–2572.

36. Landry, C. J. T.; Massa, D. J.; Teegarden, D. M.; Landry, M. R.; Henrichs, P. M.; Colby, R. H.; Long, T. E. *Macromol.* **1993,** 26, (23), 6299–6307.

37. Torrens, F.; Soria, V.; Codoner, A.; Abad, C.; Campos, A. *Eur. Polym. J.* **2006,** 42, 2807–2823.

38. Zhang, S. H.; Jin, X.; Painter, P., C.; Runt, J. *Polym.* **2004,** 45, 3933–3942.

39. Viswanathan, S.; Dadmun, M. D. *Macromol.* **2002,** 35, (13), 5049–5060.

40. Viswanathan, S.; Dadmun, M. D. *Macromol.* **2003,** 23, (9), 3196–3205.

41. Cowie, J. M. G.; Reilly, A. A. N. *Polym.* **1992,** 33, (22), 4814–4820.

42. Veytsman, B. A. *J. Phys. Chem.* **1990,** 94, 8499.

43. Panayiotou, C.; Sanchez, I. C. *J Phys. Chem.* **1991,** 95, 10090.

44. Icoz, D. Z.; Kokini, J. L. *Carbohydr. Polym.* **2007,** 70, 181–191.

45. Kuo, S.-W.; Chang, F.-C. *Macromol. Chem. Phys.* **2002,** 203, 868–878.

46. Kuo, S.-W.; Chang, F.-C. *Macromol.* **2001,** 34, (22), 7737–7743.

47. Wu, H.-D.; Chu, P. P.; Ma, C.-C. M.; Chang, F.-C. *Macromol.* **1999,** 32, (9), 3097–3105.

48. van Beek, D. J. M.; Spiering, A. J. H.; Peters, G., W. M. ; Nijenhuis, K. t.; Sijbesma, R. P. *Macromol.* **2007,** 40, 8464–8475.

49. Hameed, T.; Hussein, I. A. *Macromol. Mater. Eng.* **2004,** 289, (2), 198-203.

50. Hussein, I. A.; Williams, M. C. *Polym. Eng. Sci.* **2004,** 44, (4), 660-672.

51. Lindstrom, A.; Hakkarainen, M. *J. Polym. Sci. Pt. B-Polym. Phys.* **2007,** 45, (13), 1552-1563.

52. Feldman, K. E.; Kade, M. J.; de Greef, T. F. A.; Meijer, E. W.; Kramer, E. J.; Hawker, C. J. *Macromol.* **2008,** 41, (13), 4694–4700.

53. Park, T.; Zimmerman, S. C. *J. Am. Chem. Soc.* **2006,** 128, 13986–13987.

54. Yang, X.; Hua, F.; Yamato, K.; Ruckenstein, E.; Gong, B.; Kim, W.; Ryu, C. Y. *Angew. Chem. Int. Ed.* **2004,** 43, 6471–6474.

55. Binder, W. H.; Kunz, M. J.; Ingolic, E. *J. Polym. Sci., Part A: Polym. Chem.* **2004,** 42, 162–172.

56. van Beek, D. J. M.; Gillissen, M. A. J.; van As, B. A. C.; Palmans, A. R. A.; Sijbesma, R. P. *Macromol.* **2007,** 40, (17), 6340–6348.

57. Higley, M. N.; Pollino, J. M.; Hollembeak, E.; Weck, M. *Chemistry: A European Journal* **2005,** 11, 2946–2953.

58. Anthamatten, M. *J. Polym. Sci., Part B: Polym. Phys.* **2007,** 45, 3285–3299.

59. Park, T.; Zimmerman, S. C. *J. Am. Chem. Soc.* **2006,** 128, 11582–11590.

60. Park, Y.; Veytsman, B. A.; Coleman, M. M.; Painter, P., C. *Macromol.* **2005,** 38, (9), 3703–3707.

61. Hu, H. Y.; Painter, P., C.; Coleman, M. M. *Macromol.* **1998,** 31, 3394–3396.

62. Lee, W. B.; Elliott, R.; Katsov, K.; Fredrickson, G. H. *Macromol.* **2007,** 40, (23), 8445–8454.

63. Mather, B. D.; Baker, M. B.; Beyer, F. L.; Berg, M. A. G.; Green, M. D.; Long, T. E. *Macromol.* **2007,** 40, (19), 6834–6845.

64. Folmer, B. J. B.; Sijbesma, R. P.; Versteegen, R. M.; van der Rijt, J. A. J.; Meijer, E. W. *Adv. Mater.* **2000,** 12, (12), 874–878.

65. Wang, X.-Z.; Li, X.-Q.; Shao, X.-B.; Zhao, X.; Deng, P.; Jiang, X.-K.; Li, Z.-T.; Chen, Y.-Q. *Chemistry: A European Journal* **2003,** 9, 2904–2913.

66. ten Cate, A. T.; Dankers, P. Y. W.; Kooijman, H.; Spek, A. L.; Sijbesma, R. P.; Meijer, E. W. *J. Am. Chem. Soc.* **2003,** 125, (23), 6860–6861.

67. Sarbu, T.; Lin, K.-Y.; Spanswick, J.; Gil, R. R.; Siegwart, D. J.; Matyjaszewski, K. *Macromol.* **2004,** 37, (26), 9694–9700.

68. Karim, A.; Liu, D.-W.; Douglas, J. F.; Nakatani, A. I.; Amis, E. J. *Polym.* **2000,** 41, 8455–8458.

69. Russell, T. P.; Hadziioannou, G. *Macromol.* **1985,** 18, (1), 78–83.

70. Han, C. D.; Chun, S. B.; Hahn, S. F.; Harper, S. Q.; Savickas, P. J.; Meunier, D. M.; Li, L.; Yalcin, T. *Macromol.* **1998,** 31, (2), 394–402.

71. Roe, R.-J.; Zin, W.-C. *Macromol.* **1980,** 13, (5), 1221–1228.

72. Franke, H.; Festl, H. G.; Kratzig, E. *Colloid. Polym. Sci.* **1984,** 262, (3), 213–216.

73. Fekete, E.; Foldes, E.; Pukansky, B. *Eur. Polym. J.* **2005,** 41, 727–736.

74. Nose, T. *Polym.* **1995,** 36, (11), 2243–2248.

75. Tsai, F.-J.; Torkelson, J. M. *Macromol.* **1988,** 21, (4), 1026–1033.

76. Lin, J.-L.; Rigby, D.; Roe, R.-J. *Macromol.* **1985,** 18, (8), 1609–1611.

77. Lee, J. K.; Han, C. D. *Polym.* **1999,** 40, 6277–6296.

78. Lee, C.-F. *Polym.* **2000,** 41, 1337–1344.

79. Li, X.; Han, Y.; An, L. *Polym.* **2003,** 44, 8155–8165.

80. Pingping, Z. *Eur. Polym. J.* **1997,** 33, (3), 411–413.

81. Kalias, L.; Nysten, B.; Audinot, J.-N.; Migeon, H.-N.; Bertrand, P. *Surf. Interface Anal.* **2005,** 37, 435–443.

82. Russell, T. P.; Hjelm, R. P.; Seeger, P. A. *Macromol.* **1990,** 23, 890–893.

83. Parent, R. R.; Thompson, E. V. *J. Polym. Sci., Part B: Polym. Phys.* **1978,** 16, (10), 1829–1847.

84. Massa, D. J., Physical Properties of Blends of Polystyrene with Poly(methyl Methacrylate) and Styrene/(methyl Methacrylate) Copolymers. In *Multiphase Polymers (ACS Advances in Chemistry Series)*, Cooper, S. L.; Estes, G. M., Eds. American Chemical Society: Anaheim, California, 1979; Vol. 176, pp 433–442.

85. Kuo, C. M.; Clarson, S. J. *Macromol.* **1992,** 25, (8), 2192–2195.

86. Dong, J.; Zhang, N.; Liu, Z. *J. Appl. Polym. Sci.* **2009,** 112, 985-990.

87. Sarbu, T.; Lin, K.-Y.; Ell, J.; Siegwart, D. J.; Spanswick, J.; Matyjaszewski, K. *Macromol.* **2004,** 37, (9), 3120–3127.

88. Matyjaszewski, K.; Xia, J. *Chem. Rev.* **2001,** 101, (9), 2921–2990.

89. Keizer, H. M.; van Kessel, R.; Sijbesma, R. P.; Meijer, E. W. *Polym.* **2003,** 44, (19), 5505–5511.

90. Bernard, J.; Lortie, F.; Fenet, B. *Macromol. Rapid Commun.* **2009,** 30, (2), 83–88.

91. Chai, Z.; Sun, R.; Li, S.; Karasz, F. E. *Macromol.* **1995,** 28, (7), 2297-2302.

92. Li, M.; Yamato, K.; Ferguson, J. S.; Gong, B. *J. Am. Chem. Soc.* **2006,** 128, 12628–12629.

93. Sijbesma, R. P.; Beijer, F. H.; Brunsveld, L.; Folmer, B. J. B.; Hirschberg, J. H. K. K.; Lange, R. F. M.; Lowe, J. K. L.; Meijer, E. W. *Science* **1997,** 278, (5343), 1601-1604.

94. Liu, X. Y.; Gao, G. Q.; Dong, L.; Ye, G. D.; Gu, Y. *Polym. Adv. Technol.* **2009,** 20, (4), 362–366.

95. Cao, Y.; Wang, Y.; Li, B. T.; Tang, L. M. *Chin. J. Polym. Sci.* **2008,** 26, (6), 767–774.

96. Tang, L. M.; Wang, Y.; Qiu, Y. P.; Guan, S. Y. *Acta Polym. Sin.* **2009**, (1), 93–96.

97. Sperling, L. H., *Introduction to Physical Polymer Science*. 3rd ed.; Wiley-Interscience: New York, 2001.

98. Xiang, M.; Jiang, M.; Zhang, Y.; Wu, C. *Macromol.* **1997,** 30, (18), 5339–5344.

99. Zhu, B.; He, Y.; Yoshie, N.; Asakawa, N.; Inoue, Y. *Macromol.* **2004,** 37, (9), 3257–3266.

100. Dreezen, G.; Groeninckx, G.; Swier, S.; Van Mele, B. *Polym.* **2001,** 42, 1449–1459.

101. Lu, H.; Zheng, S.; Tian, G. *Polym.* **2004,** 45, 2897–2909.

102. Tang, M.; Liau, W.-R. *Eur. Polym. J.* **2000,** 36, 2597–2603.

103. Belorgey, G.; Prud'homme, R. E. *J. Polym. Sci.* **1982,** 20, 191.

104. Belorgey, G.; Aubin, M.; Prud'homme, R. E. *Polym.* **1982,** 23, 1051.

105. Robeson, L. M., *Polymer Blends: A Comprehensive Review*. Hanser Gardner Publications, Inc.: Cincinatti, 2007.

106. Yang, Z.; Zheng, S. Y.; Harrison, W. J.; Harder, J.; Wen, X. X.; Gelovani, J. G.; Qiao, A.; Li, C. *Biomacromol.* **2007,** 8, (11), 3422-3428.

Appendix A

This appendix contains a summary of the reaction conditions and resulting molecular weights and polydispersities for ATRP polymerizations with UPy-bromoisobutyrate initiator, and the subsequent ATRC coupling reactions. In cases where resulting polymers displayed a bimodal molecular weight distribution, molecular weight and polydispersity are not reported for overlapping peaks. Shaded rows indicate coupling reactions.

Table A-1: Summary of reaction conditions for ATRP/ATRC reactions using UPy-bromoisobutyrate initiator.

CuBr (mmol)	$CuBr_2$ (mmol)	nano-Cu (mmol)	Monomer (mmol)	PMDETA (mmol)	Initiator (mmol)	Temp (°C)	Time	M_n (g/mol)	PDI
1.07	0.05	--	S-174	1.05	1.06	85	2 hr	27,300	2.24
0.53	0.03	--	S-87	0.53	0.53	90	2 hr	bimodal	
1.78	0.09	--	S-87	1.82	0.44	90	2 hr	27,200	1.24

CuBr (mmol)	$CuBr_2$ (mmol)	nano-Cu (mmol)	Monomer (mmol)	PMDETA (mmol)	Initiator (mmol)	Temp (°C)	Time	M_n (g/mol)	PDI
0.42	--	1.44	--	0.72	0.04 UPSBr 27,200 g/mol	75	4 hr	bimodal, incomplete coupling	
1.77	0.09	--	S-87	1.82	0.55	90	1 hr	bimodal	
1.14	0.06	--	S-87	1.14	0.53	90	2 hr	7,600	1.39
0.57	--	1.93	--	1.20	0.03 UPSBr 7,600 g/mol	75	24 hr	15,000	1.07
0.53	0.03	--	S-87	0.53	0.53	87	2 hr	3,400	1.29
2.61	0.13	--	S-435	2.64	2.63	70	2 hr	13,600	1.89
1.78	0.10	--	MMA-74	1.91	0.53	58	2 hr	18,000	4.10
1.75	0.10	--	MMA-74	1.83	0.53	60	1 hr	26,900	3.41
1.31	0.13	--	MMA-74	1.39	0.84	55	1 hr	13,200	3.01
0.08	--	0.30	--	0.19	0.08 UPMMABr 13,200 g/mol	70	24 hr	23,000	2.82

CuBr (mmol)	$CuBr_2$ (mmol)	nano-Cu (mmol)	Monomer (mmol)	PMDETA (mmol)	Initiator (mmol)	Temp (°C)	Time	M_n (g/mol)	PDI
0.54	0.03	--	S-87	0.53	0.55	85	2 hr	11,400 4,800	1.06 1.10
0.88	0.19	--	MMA-74	0.91	1.04	55	1 hr	6,300	1.65
0.13	--	0.42	--	0.24	0.11 UPMMABr 6,300 g/mol	80	19 hr	8,400 20,700	2.3 1.75
1.55	0.08	--	S-261	1.58	1.58	85	2 hr	2,400	1.11
0.51	--	1.79	--	0.96	0.44 UPSBr 2,400 g/mol	82	24 hr	9,700	1.60
1.76	0.36	--	MMA-150	1.92	2.12	50	1 hr	6,000	2.36